LOW COST AND PRACTICAL SOLAR FRUIT DRYING SYSTEM FOR DEVELOPING COUNTRIES

FINAL REPORT
Contract No. DAN-5053-G-SS
(October 1987 - June 1989)

U. S. AGENCY FOR INTERNATIONAL DEVELOPMENT
Washington, D. C.

By

D. Y. Goswami, A. Shahbazi, A. Lavania and M. Mahmood

North Carolina A & T State University
Greensboro, N. C. 27411

November, 1989

TABLE OF CONTENTS

CHAPTER 1
INTRODUCTION

Drying involves the process of removing moisture from agricultural crops and products for high quality and safe storage. The process includes both heat and mass transfer. Drying is accomplished by solar energy or other resources such as natural gas, propane, oil and wood. Utilization of solar energy for drying is the process in which solar radiation is converted to thermal energy.

Most driers in the U.S.A are run on fossil fuels. Whenever solar energy is utilized, it is in the form of supplemental heat. The main reason for the low use of solar energy is that long term thermal storage of solar energy has been impractical or inefficient. However in developing countries where fossil fuel is a rare commodity, solar energy holds much greater potential.

Solar dryers can be classified into two categories, i.e. natural convection dryers and forced convection dryers. Natural convection dryers do not require any mechanical or electrical power to circulate the air through the product. Natural or forced convection dryers can also be classified into three categories, depending upon their heating modes.

1. Direct solar dryers in which the product directly collects energy from the sun.

2. Indirect solar dryers in which the product is dried with warm air heated separately by solar air heaters. The product to be dried does not see the sun directly in this case. Figure 1.1 shows a simple solar dryer that is a combination of the direct and the indirect types.

3. Industrial type dryers in which the system utilizes solar and non-solar heating energy. These dryers usually are of continuous type and have large capacities. Figure 1.2 shows an industrial

type parallel flow fruit dryer.

A greenhouse type of solar drier can be set up as an indirect or a direct drier depending on whether a layer of opaque absorber is placed between the outer transparent glazing and the product, or not. Such a dryer can be set up to work in the natural convection or the forced convection mode. For drying purposes, the amount of solar energy collected is an important criterion. The geometric shape of the greenhouse determines the amount of energy collected at any location. It was estimated that a geodesic dome performs better than other geometric shapes. Figure 1.3 shows the structure of a geodesic dome. A complete design procedure for geodesic dome greenhouse is given in Chapter 3. A geodesic dome type of solar fruit dryer was designed and constructed. It is located at the Enviromental Laboratory at the N.C.A&T State University farm. In this study experiments on drying grapes were conducted using these facilities. Complete data were recorded using a portable automatic data acquisition system. The data obtained was plotted and compared with theoritical simulation results.

CHAPTER 2
LITERATURE REVIEW

In direct solar dryers, the material is placed in shallow layers on trays inside a hot box and is directly exposed to solar radiation. A dryer of this type consists of an enclosure with a transparent cover which produces a greenhouse environment inside the enclosure. These dryers are sometimes called cabinet dryers. In this case one side of the cabinet is glazed to admit solar radiation. This radiation is then converted to low grade heat which heats up the air and the product inside the cabinet. The solar heat causes the product moisture to evaporate and move away with the circulating air. Air circulation is produced naturally by the temperature difference between the hot air inside and the cooler air outside. Drying is less efficient in these units and takes more time. The efficiency can be significantly improved by adding a mechanical fan or blower to these units. The fan forces the warm air through the product and moves the moist air out of the cabinet. Lawand [1] reported on a cabinet dryer which had 1.3 sq.meter drying bed. This dryer reduced the drying time of various fruits by 50% to 65% over open-air sun drying.

Usually, direct solar dryers are relatively small. They come in many different designs and are extensively used by individual farmers or families of farmers in developing countries. Large direct dryers for use in commercial operation, should be built as greenhouse- type structures. Some advantages of greenhouse dryers over cabinet dryers are their large capacities and greater degree of control over the drying process.

Gutierrez [2] used a 10x12 foot glass house for drying fruits. He used a forced-air configuration in which the greenhouse air enters under the thermal absorber, travels to the back of the greenhouse and then rises to the top. The duct at the top brings the air down and forces it through the fruit trays. This configuration provides a temperature rise of 20-25 F above ambient. This drying facility can easily be scaled up to a commercial size operation according to Gutierrez. Another greenhouse-type solar dryer was desiged and studied by Huang [3]. The unit is made up of a large multidirectional solar collector with a transparent cover at the outside and interchangeable inner chambers with black absorbing bodies for drying and curing purposes. Two types of drying configurations can be placed inside the greenhouse; (a) a per-

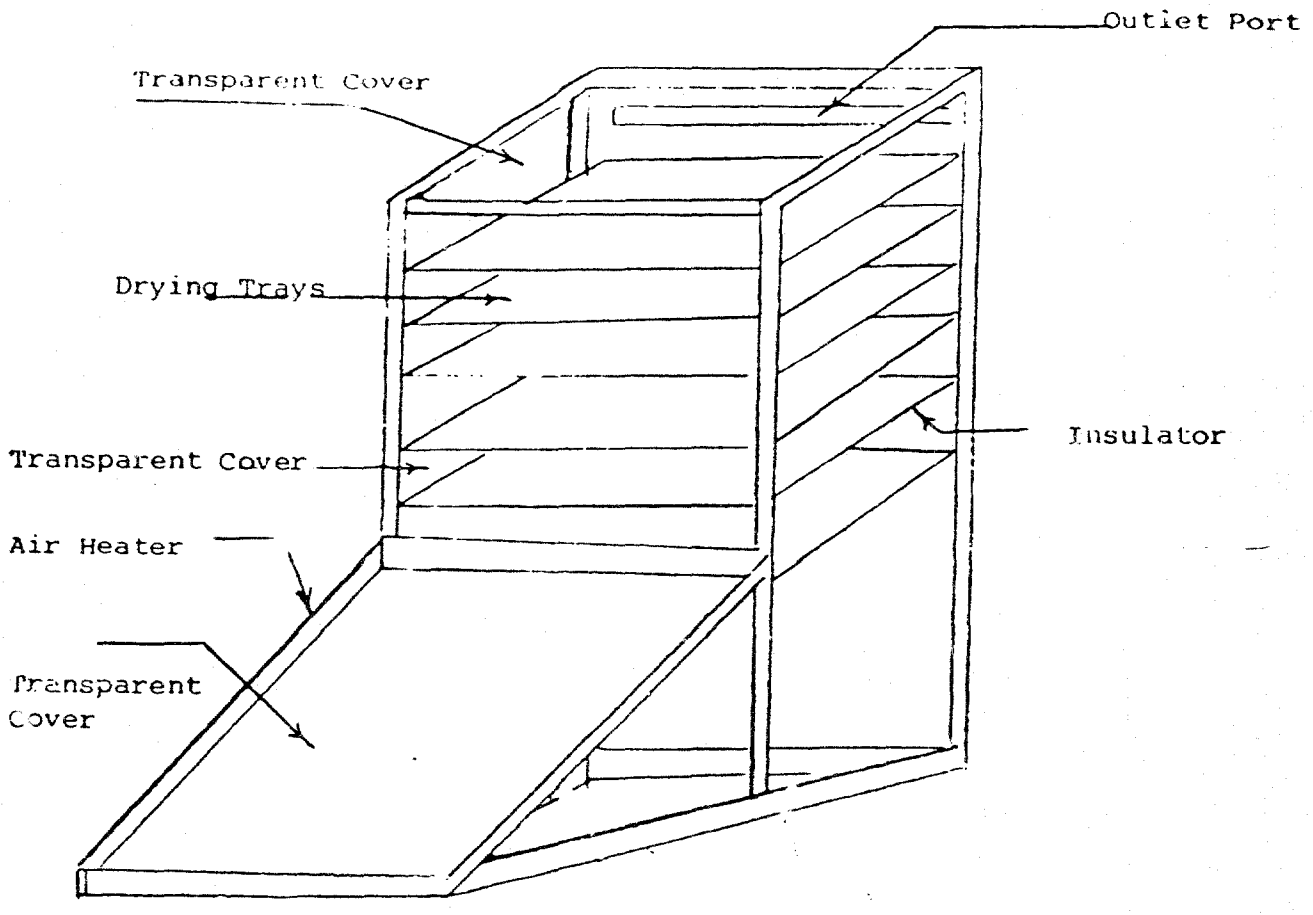

Fig. 1.1 Cabinet type Solar Dryer with separate air heater

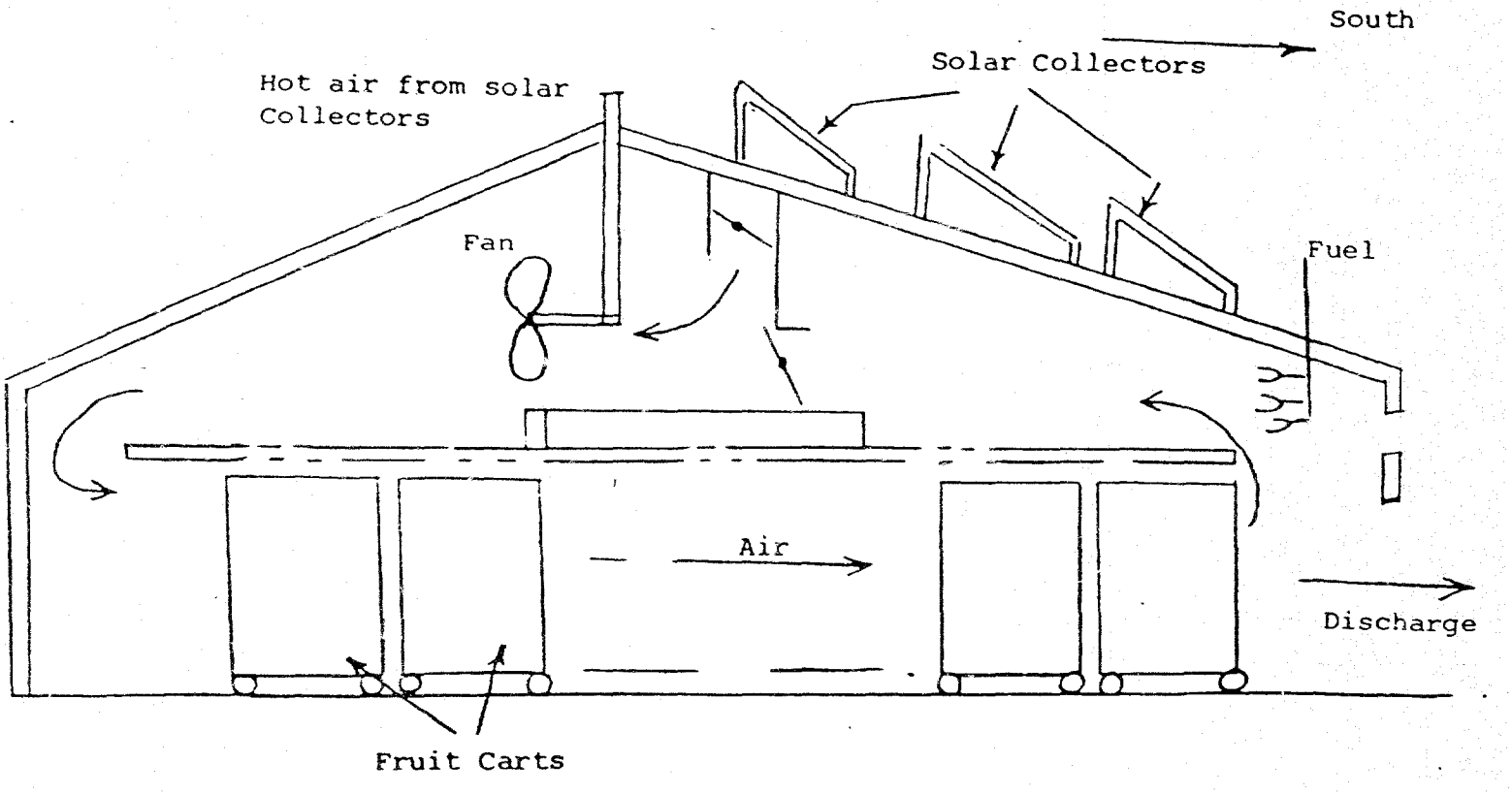

Fig. 1.2 Industrial type parallel flow dryer with solar collectors

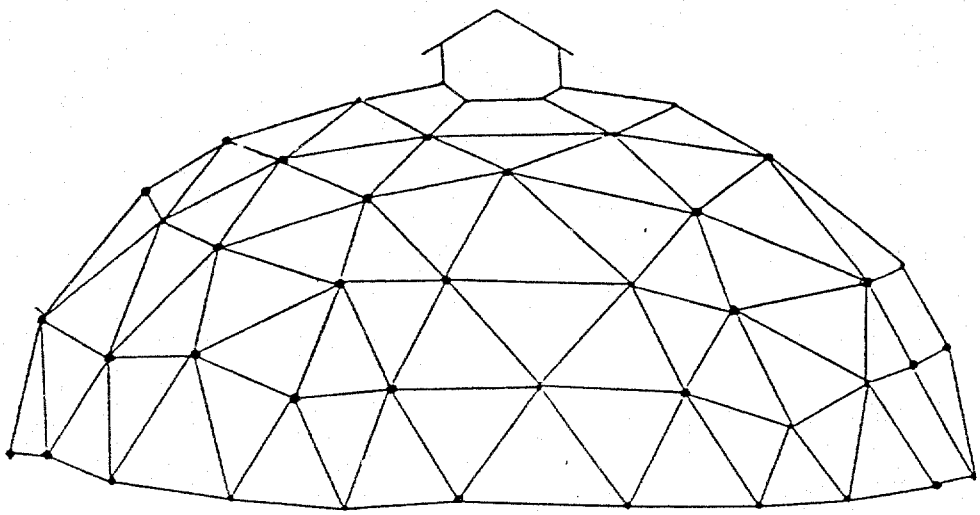

(a) Perspective view of dome.

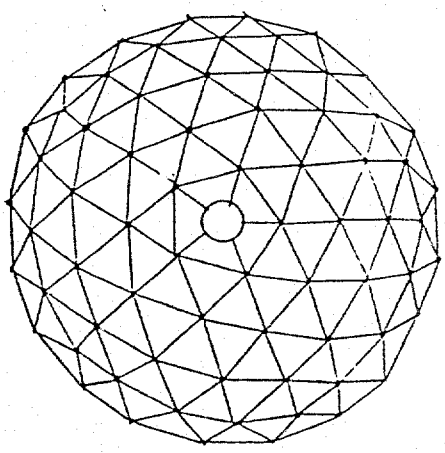

(b) Top view of dome.

Fig. 1.3 Geodesic - dome solar fruit dryer.

forated and rotating drum, used for drying grain and peanuts, and (b) a bulk rack for curing tobacco. The bulk rack can be modified for drying fruits. Curing tobacco in this facility provides quality tobacco with 47 to 54% fuel saving over the conventional bulk-barn curing.

In Indirect solar dryers, the fruit is not exposed to direct solar radiation. Most designs in this category are made up of a hot air solar collection system and a drying chamber. The chamber is usually insulated and contains a series of screened trays to support the drying fruits. The hot air from the solar collectors is fed into the drying chamber via an inlet port at the bottom of the chamber. The hot air ascends up the chamber drying the fruits and exits from the exhaust port at the top of the drying chamber. These dryers result in higher temperature than the direct dryers (cabinet or open air sun drying). A disadvantage of these dryer is that it is difficult to maintain a constant operating condition within the drying chamber because of fluctuation in the temperature of the air leaving the solar collector. The air is circulated through the system either by natural convection or by means of a mechanical blower.

In Industrial type dryers, the product can be dried by solar energy as well as by fossil fuels. These dryers normally have large capacity, run continuously and provide the shortest drying time. Some of the earlier investigations on energy efficient dehydrators were performed by Cruss and Christie [4]. They used a tunnel dryer which consisted of a long rectangular structure. The carts containing the fruits would enter from one end of the structure,moving at a constant speed, and exit at the other end. Heated air was used as a substitute for sun drying of prunes in this experiment. In 1929, Christie and Nichols [5] studied the effect of air temperature, humidity, fruit variety, pretreatment of the fruit and air speed on the drying time. Mark [6] showed that non-uniform flow of air has significant effect on the fruits leaving the tunnel with variable moisture content. Most investigators agreed that relative humidities of the exhaust air in counter current flow tunnels should be in the range of 35%-40%.

Gentry [7] demonstrated that concurrent (parallel) flow operation of a tunnel designed for traditional counter flow operation would significantly decrease drying time. Since then, many of the older tunnels have been converted to concurrent flow operation and new tunnels are designed for this mode of operation. Robert [8] studied drying of prunes in parallel flow operation and found 33% faster drying than countercurrent drying with less fuel consumption. Most of the earlier designs were

based on the Rodda and Gentry [9] work. Air flow uniformity was not incorporated as a design consideration, but some of the tunnels had turning vanes in the top airchamber of the dehydrator.

Cheng [10] analyzed the effect of a suction slot located just above the front cars. The flow diverters were arranged such that the air is directed upward, allowing the first set of vanes to turn the flow 90 degrees while leaving enough space to locate the lower set of vanes above the pathway of the cars. Croh [11] suggested that increased recirculation anduse of heat exchangers would reduce energy use. In 1980, Carnegie [12] analyzed the effectiveness of various heat exchanger systems for recovering heat from exhaust air. Thompson [13] discussed the thermal losses associated with tunnel dehydrators and the methods to minimize these losses. The main area of heat losses are exhaust air, burner inefficiency and air leaks. Heat lost by conduction through the wall and by hot fruits and trays leaving the tunnel is relatively small. A heat shield was placed by Thompson behind the rear wall(burner) to stop convective heat loss and also to absorb radiant heat from the heat from the steel plate. Adams [14] conducted experiments on the performance of concurrent dehydrator maintaining more uniform flow using flow diverters and turning vanes.

Thermal response of a solar drier can be analyzed by using the analogy between electrical current flow and heat flow. This method, called the Thermal Circuit Method has been used by many investigators (15-17) to study rates of heat flow through walls and roofs subjected to unsteady atmospheric conditions. Buchberg (18) used this method as an analog computer technique to study the temperature-time response os a structure the rate of heat transfer of the space in the structure. Jensen and Lieberman (19) discussed the application of an Electrical Circuit Analysis Program (ECAP) in the analysis of thermal systems. Huang et. al. (20-23) used PCAP (Princeton Circuit Analysis Program), which is a modified version of ECAP, to study the dynamic system response of agricultural thermal systems. Later, Huang and El Sheik (24) used this technique to study the thermal response of a Greenhouse Solar Drying System for dryng peanuts and grains. Results showed good agreement between the computer predictions and the measured thermal behaviour of the solar drier. Ozisic and Huang (25) applied the same technique to study the heat and mass transfer in grain drying in a greenhouse solar drying system using rotary drums in the greenhouse as solar collectors.

CHAPTER 3
Design and Fabrication of Geodesic Dome

3.1 Introduction

This chapter draws heavily on the material presented in references [26]-[28]. Dome is a multifaced polyhedron in which all the vertices lie on the surface of a sphere. Domes are developed from the tetrahedron and the icosahedron. Most of the domes are derived from icosahedron. The triangles of the icosahedron are subdivided into smaller triangles to form a geodesic dome. The geodesic dome has produced a building technology which can be applied to many shapes.

Dome (frame type) construction integrates the structure into a continuous surface and distributes the surface forces by triangulating the convex curve. In addition to being light weight, the dome structure has the following advantages.

1. The entire structure is in a state of compression.

2. Trianguler elements of the geodesic dome provides lateral stability.

3.2 Materials for the dome frame

Possible materials for the dome frame are:

(a) Wood, Bamboo
(b) PVC Plastic pipe.
(c) Aluminum.

(a) Wood is strong, relatively cheap, light weight and can be cut out and assembled with hand tools. Wood can be cut easily at any angle, and shape. To increase the life of wood a coat of wood preservative such as creosote oil helps. An important advantage of wood is that it is available in all parts of the world. Bamboo may be a more appropriate choice in some developing countries.

(b) PVC Plastic pipe is not strong for a framework, because it gets brittle and shows cracks after some time.

(c) Aluminum is two or three times more expensive than other materials. If lightness and corrosion resistance are important, it might be worth it.

(d) Electrical Conduit pipe with the ends crimped and drilled is probably the cheapest and the simplest frame in the U.S.A. An eye bolt can be used at the hubs. Unavailability of electrical conduit pipe in some countries is a drawback.

3.3 Design specifications

Figures 3.1a to 3.1f explain the terminology used in the design and construction of geodesic domes.

The following specifications were used for the design of a dome for testing:

Diameter : 288 inches
Height : 117 inches
3/8 sphere, 4 frequency, icosahedron, Geodesic type
Standard values of chord factor(cf), axial angle(AA),
face angle(FA) and dihedral angle(DA)

Figures 3.2 and 3.3 show the arrangement of members for a 3/8, 4 frequency , icosahedron geodesic dome. The length and angles of the members for the above specification are calculated as shown below. The values are given in the tables 3.1 to 3.6.

Member-B

AA= 180 - CA / 2
CA= 180 - (AA1 -AA2)
cf= 2(Sin CA/2)
L= cf . r
Where AA is axial angle
CA is central angle

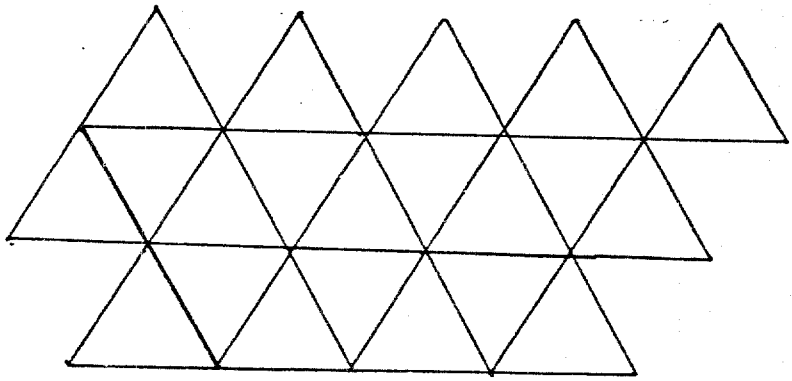

(a) Geodesic

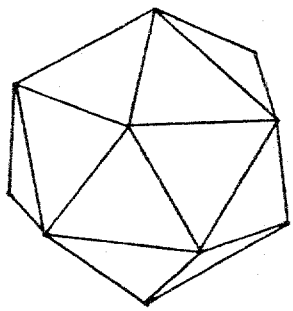

(b) Icosahedron

Fig: 3.1(a,b) Basic definitions of Geodesic Math.

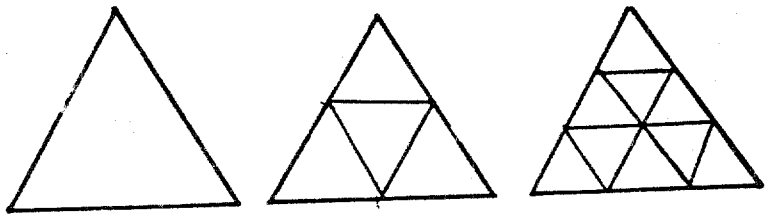

(c) Frequency

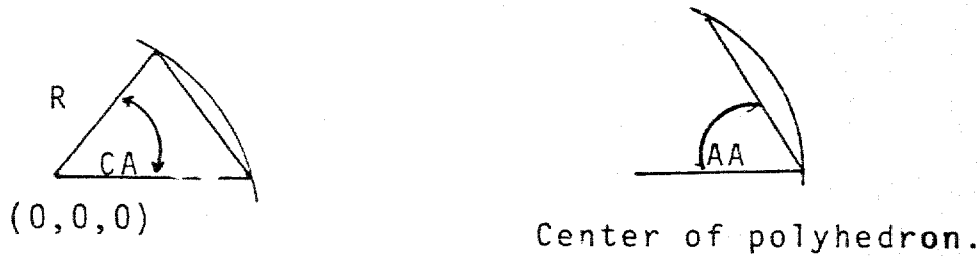

(d) Central Angle and Axial Angle

(e) Face Angle and Dihedral Angle

Fig: 3.1(c,d,e) Basic definations of Geodesic Math.

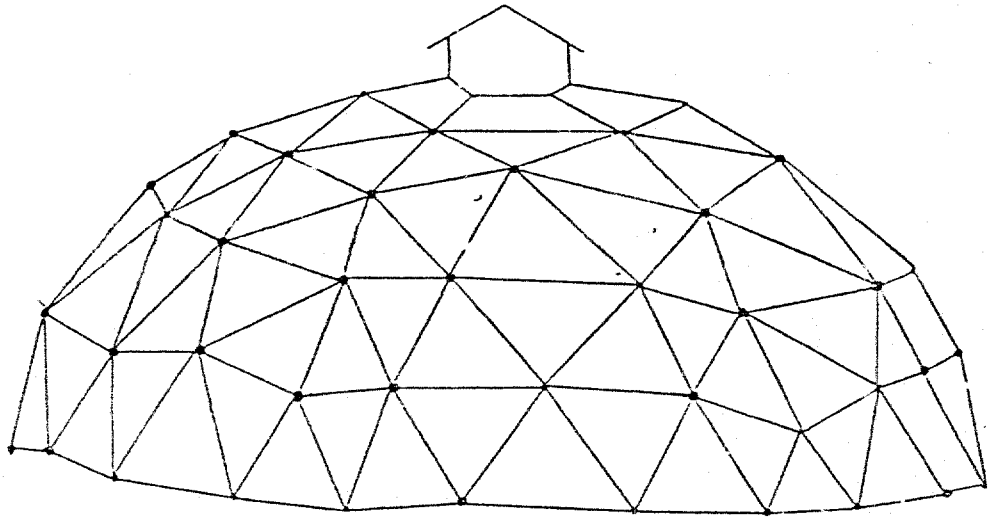

3/8 Sphere

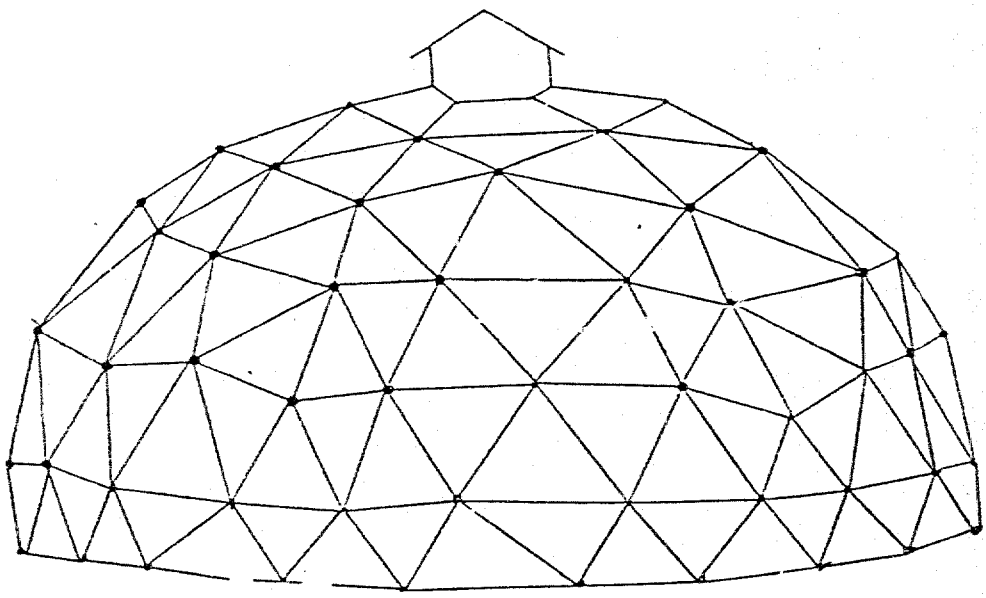

5/8 Sphere

Fig: 3.1 f Shows two ways of geodesic dome structure.

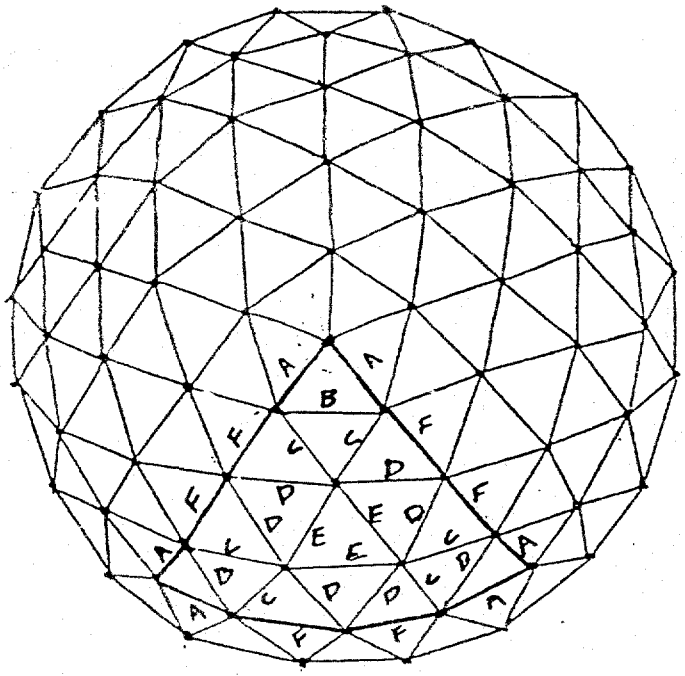

Fig: 3.2 4-frequency icosahedron of 3/8 sphere geodesic dome.

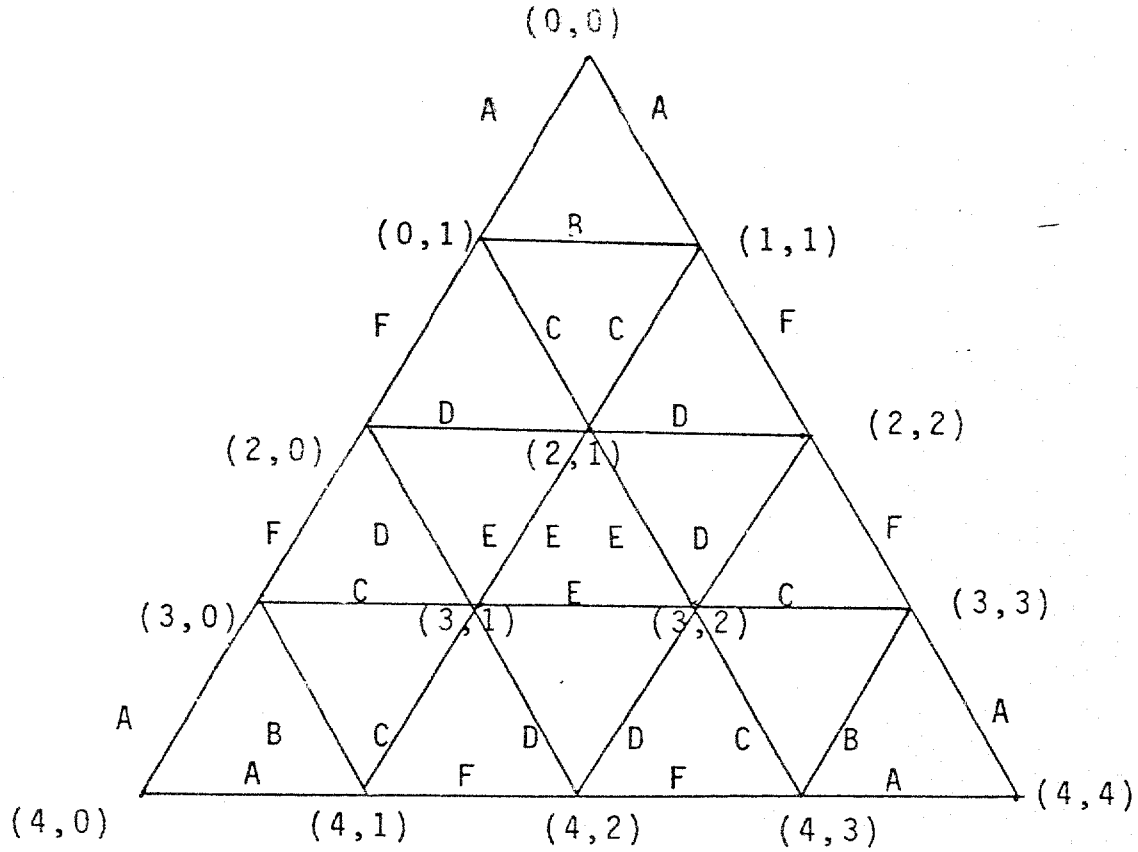

Fig: 3.3 4-frequency faces of 3/8, 4-frequency Geodesic dome.

L= cf . r = (Ø.2952) . (13)=3.838'

Where L is the length of a member and r is the radius of the sphere.

Table 3.1 Calculated values of wood members.

Angle Name	Nodes			Angle degree
AA	Ø,Ø	1,Ø	1,1	(81.52)
FA	1,1	Ø,Ø	1,Ø	(71.33)
DA	1,1	1,Ø		(172.19)

Member-D

cf 2,1 2,Ø Ø.312868

L= cf . r = (Ø.3128) . (13) = 4.Ø6'

Table 3.2 Calculated values of wood members.

Angle Name	Nodes			Angle degrees
AA	Ø,Ø	2,Ø	2,1	(8Ø.99)
FA	2,1	1,Ø	2,Ø	(63.66)
FA	2,1	3,1	2,Ø	(58.77)
DA	2,1	2,Ø		(169.98)

Member-C

cf 3,1 3,Ø Ø.29453

L=cf . r = (Ø.2945) . (13) = 3.28'

Table 3.3 Calculated value of wood member.

Angle Name	Nodes			Angle degrees
AA	Ø,Ø	3,Ø		(81.35)
FA	3,1	2,Ø	3,Ø	(57.53)
FA	3.1	4,1	3,Ø	(59.92)
DA	3,1	3,Ø		(169.61)

Member-E

cf 3,2 3,1 Ø.3249

L = cf . r = (Ø.3249) . (13) = 4.22'

Table 3.4 Calculated value of wood members.

Angle Name	Nodes			Angle degrees
AA	Ø,Ø	3,1	3,2	(8Ø.65)
FA	3,2	2,1	3,1	(59.99)
FA	3,2	4,2	3,1	(62.56)
DA	3,2	3,1		(169.64)

Member-A

cf 4,1 4,Ø Ø.25318

L= cf . r = (Ø.2531) . (13) = 3.3Ø'

Table 3.5 Calculated value of wood members.

Angle Name	Nodes			Angle degrees
AA	Ø,Ø	4,Ø	4,1	(82.77)
FA	4,1	3,Ø	4,Ø	(54.33)
DA	4,1	4,Ø		(169.49)

Member-F

cf 4,2 4,1 Ø.29858

L= cf . r = (Ø.2985).(13) = 3.86'

Table 3.6 Calculated values of wood members.

Angle Name	Nodes			Angle degrees
AA	Ø,Ø	4,4	4,2	(81.42)
FA	4,2	3,1	4,1	(58.79)
DA	4,2	4,1		(169.5Ø)

3.4 Fabrication and Instalation

As shown in figure 3.4, the designed dome structure consists of ten hexagons, five pentagons and a five corner top structure. Using the dimensions of A,B,C,D,E and F as calculated above, required dimensions for all the members of dome were specified. Details of the dimensions are given in tables 3.7 to 3.13 and figures 3.6 to 3.9. Type of members and accessories used are shown in figure 3.5.

Table 3.7 Data for the members of the pentagons (Figure 3.6)

Member	Type	Dimension				Quantity
		L1	L2	W	t	(For 5 Pentagons)
A1	A	2"	3'-6"	1'-5"	1"	25
A2	B	2"	3'-1"	1'-5"	1"	25

Table:3.8 Hub Sizes for five Pentagons

Hub	Type	Dimensions		Quantity
		D	t	(For 5 Pentagons)
A3	E	6"	1/2"	5
A4	G	1"	1/2"	5
A5	F	6"	1/2"	1Ø
A6	E	6"	1/2"	15

Table:3.9 Data for Members of the Hexagons (Figure 3.7)

Member	Type	Dimension				Quantity
		L1	L2	W	t	(For 5 Hexagons)
B1	A	2"	4'-2"	1'-5"	1"	1Ø
B2	B	2"	3'-8"	1'-5"	1"	5Ø
B3	B	2"	4'-Ø6"	1'-5"	1"	2Ø
B4	B	2"	4'-Ø6"	1'-5"	1"	2Ø
B5	B	2"	3'-8"	1'-5"	1"	2Ø

Table 3.1Ø Hub Sizes for the Hexagons (Figure 3.7)

Member	Type	Dimension		Quantity
		D	t	(For 5 Hexagons)
A4	E	6"	1/2"	5
A3	G	1"	1/2"	5
A6	F	6"	1/2"	1Ø
A7	E	6"	1/2"	1Ø

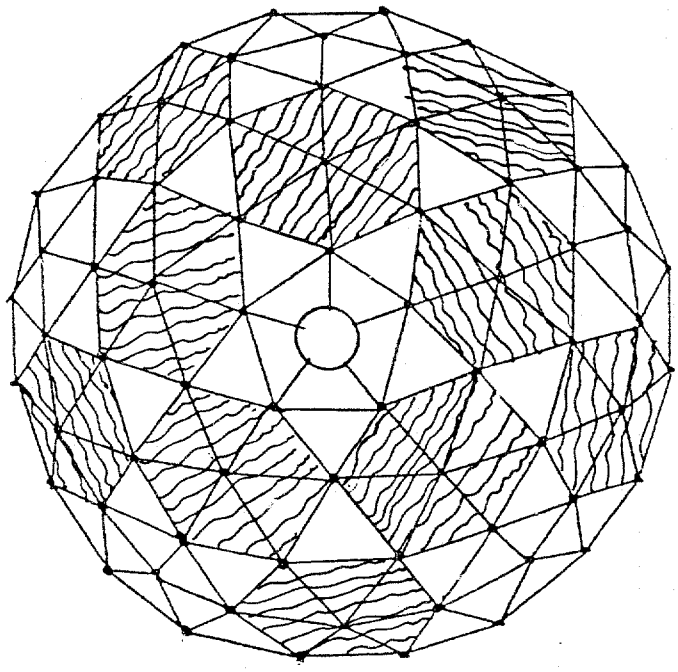

Fig: 3.4 Top view of dome, shows number of pentagons hexagons and top frame.

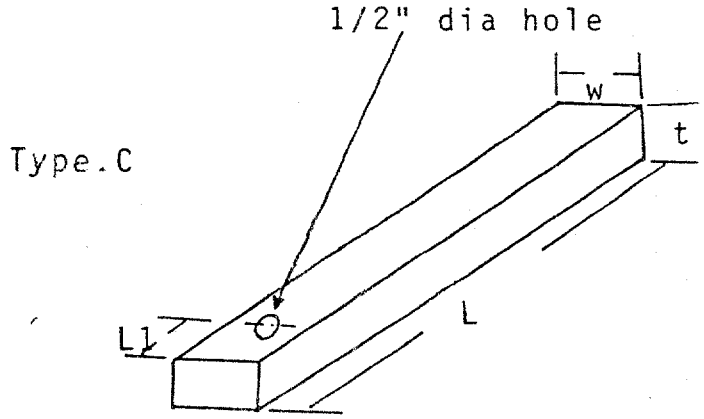

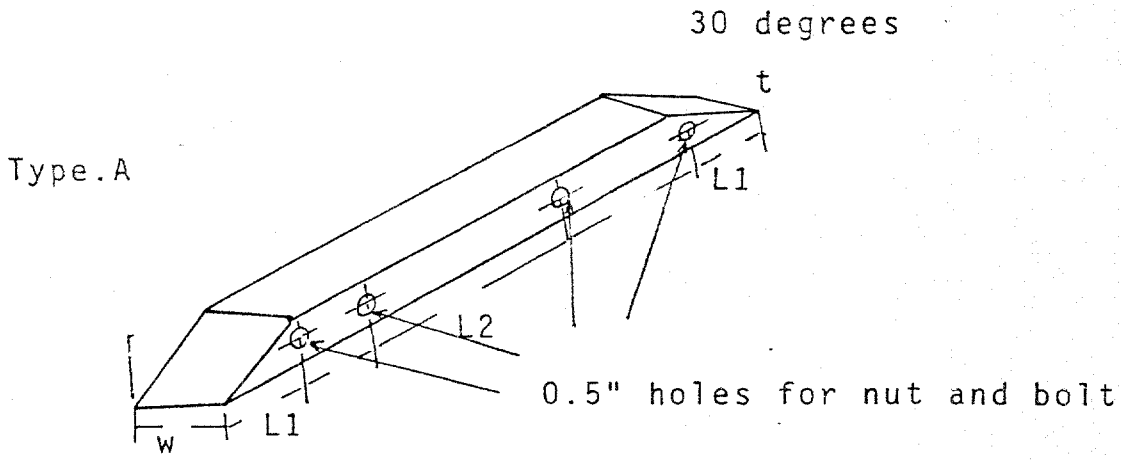

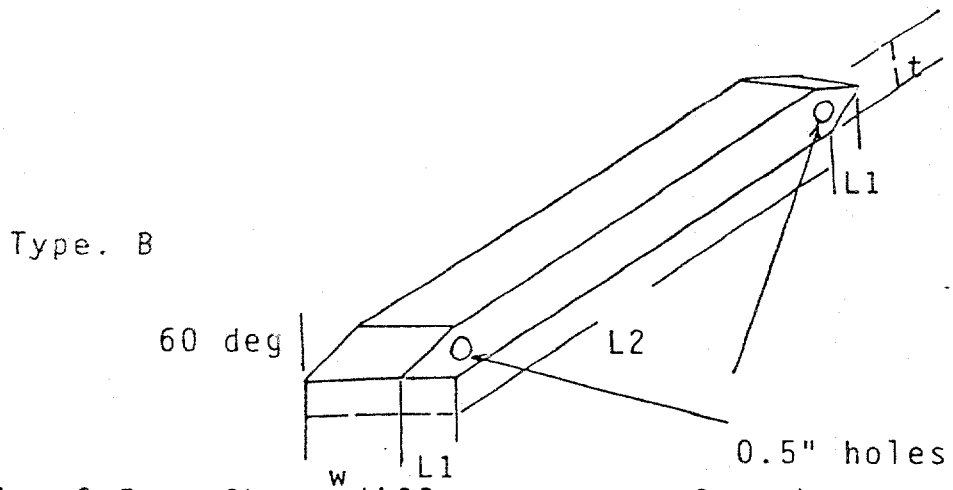

Fig: 3.5 a Shows different type of members.

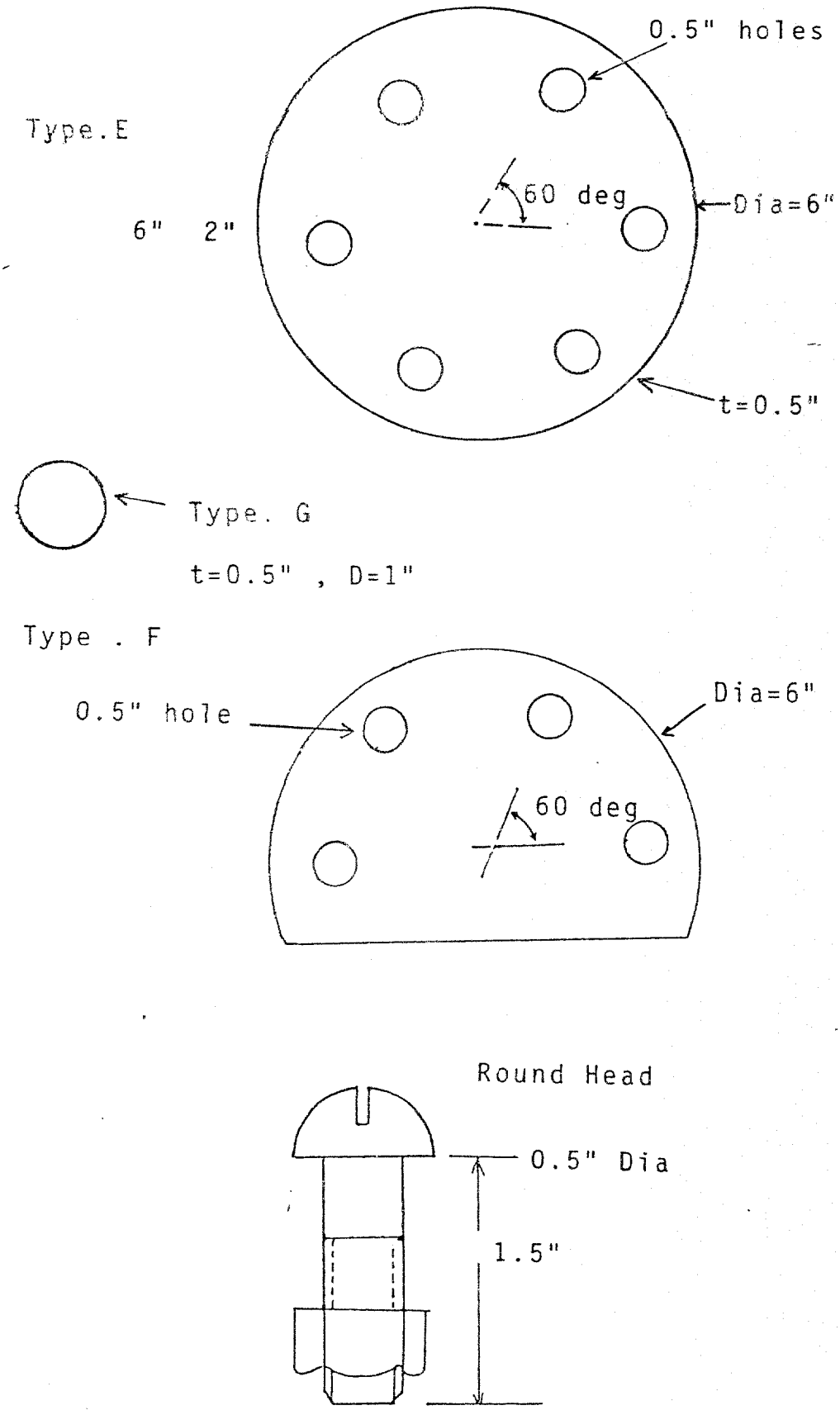

Fig: 3.5 b Shows different type of accessories.

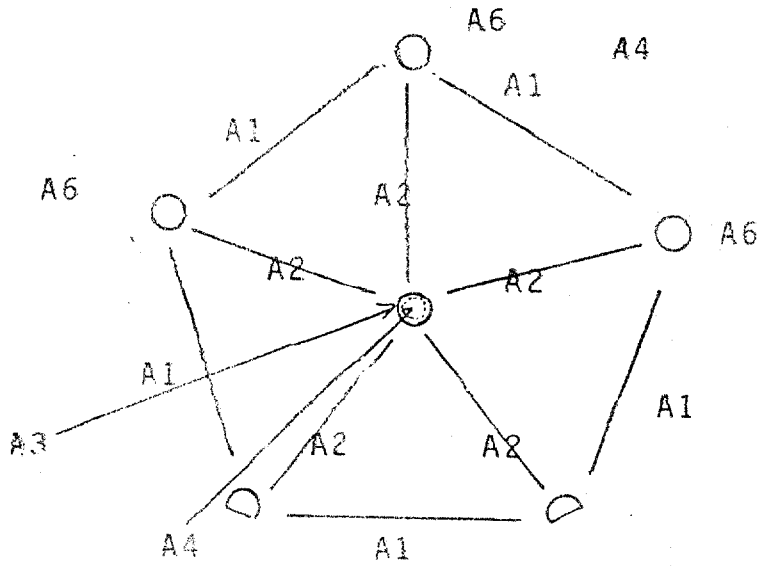

A5

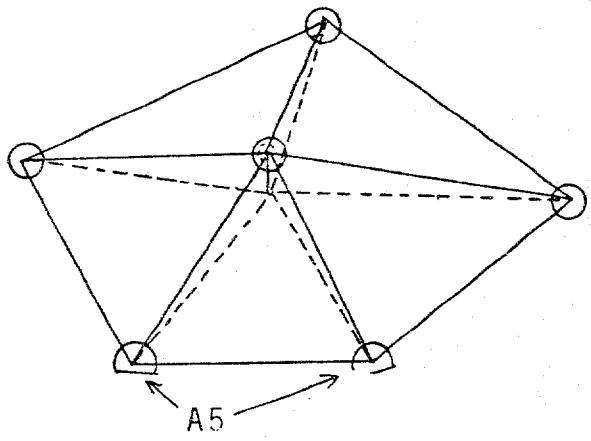

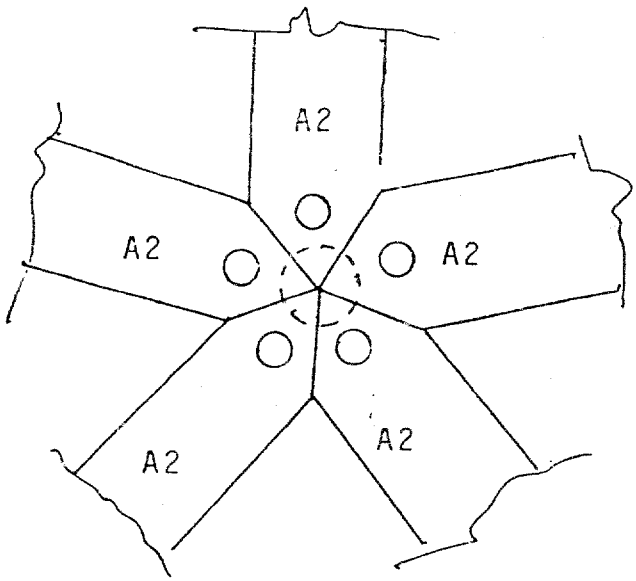

Detail of joint

Fig: 3.6 Arrangement of wood members for pentagon

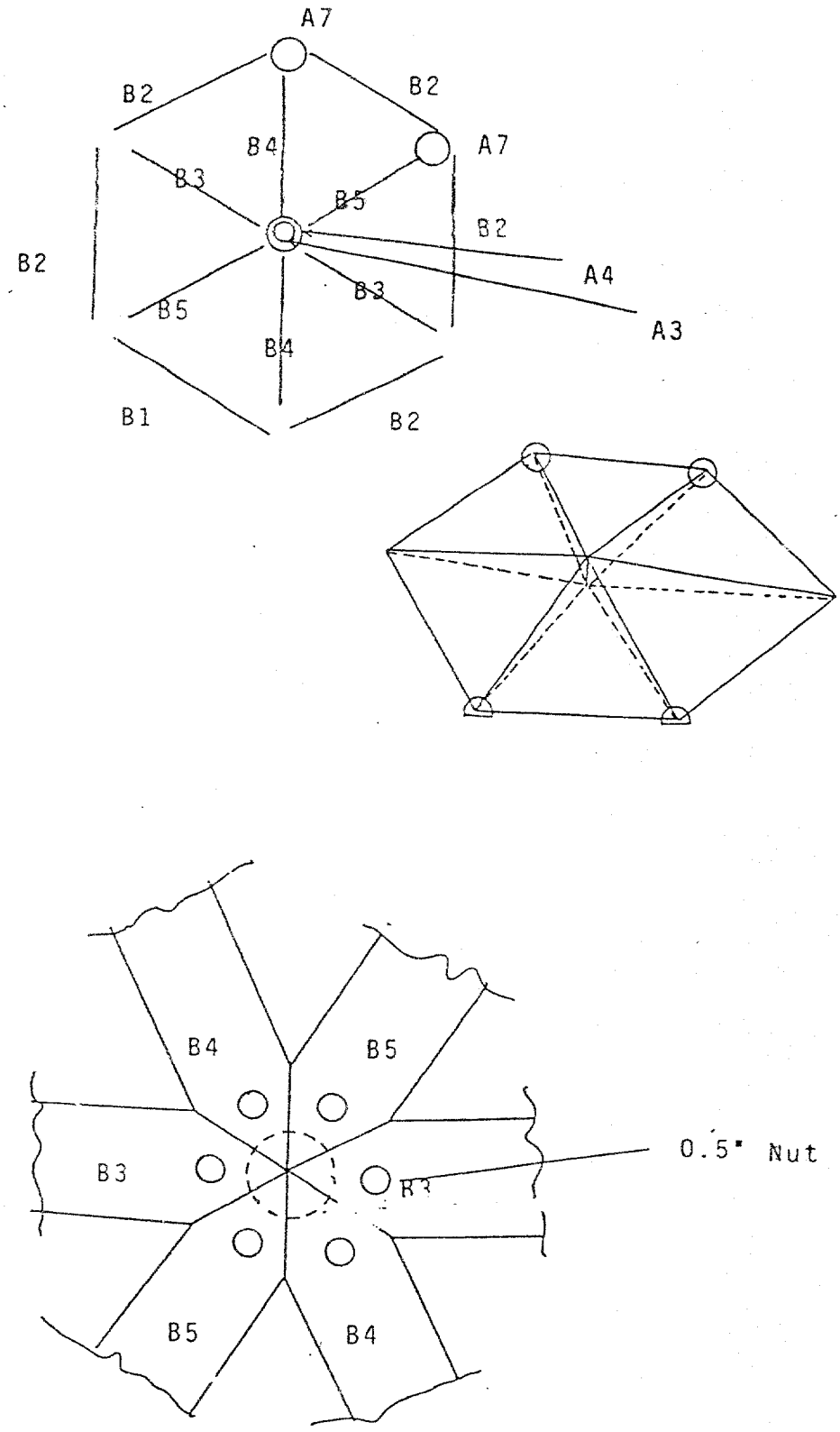

Fig: 3.7 Arrangement of wood members for a hexagon

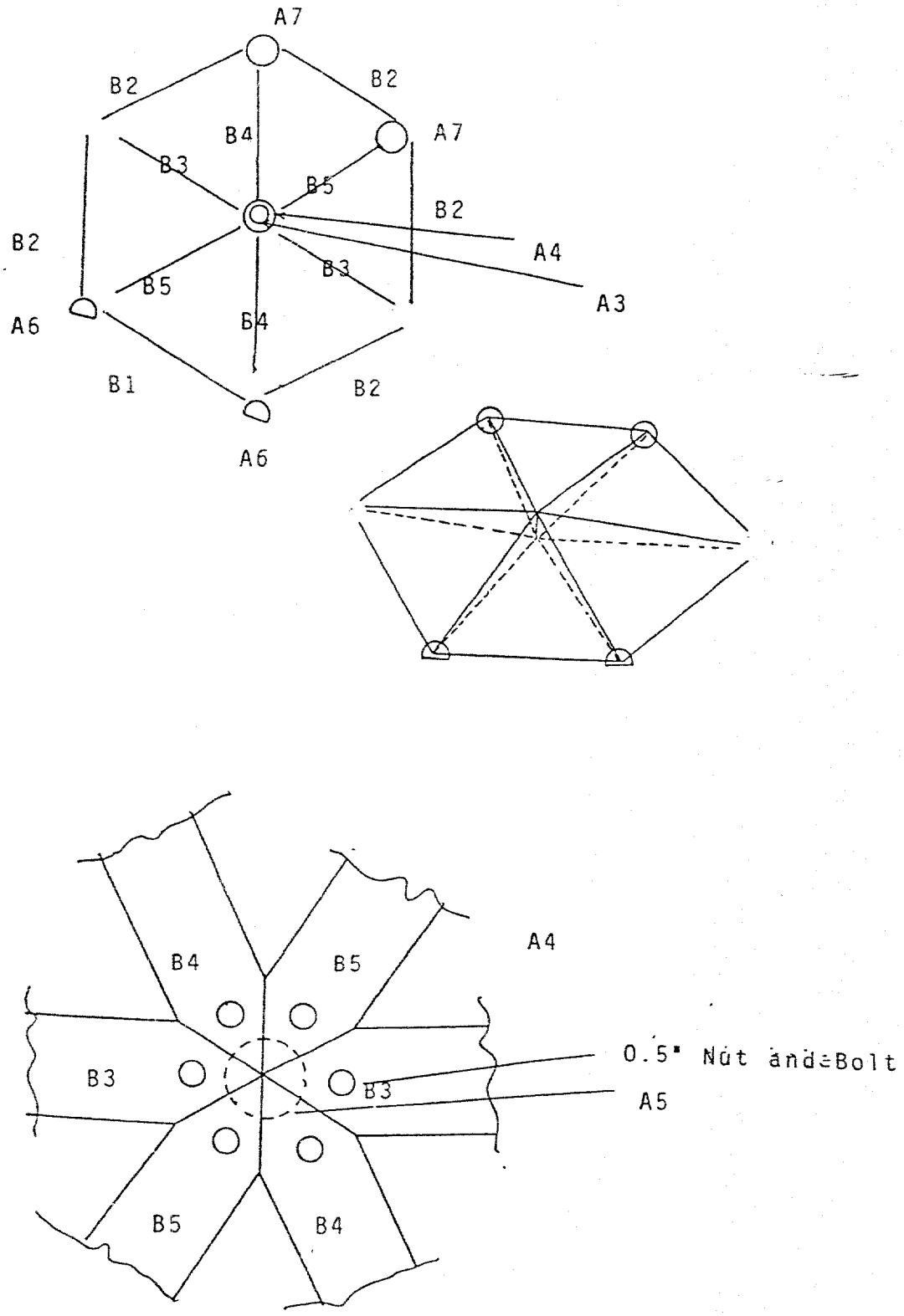

Fig: 3.8 Arrangement of wood members for a hexogon.

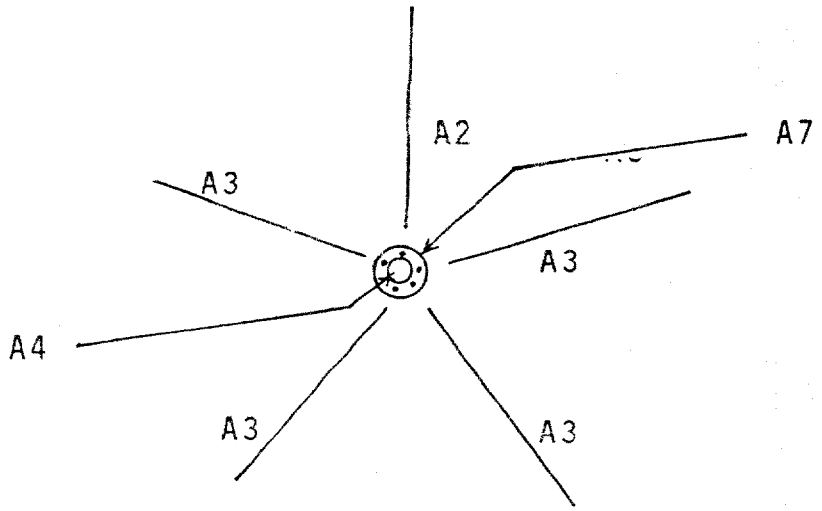

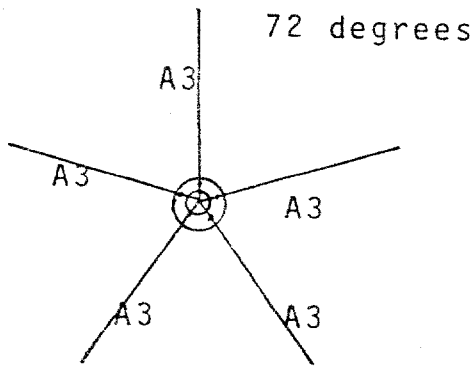

Fig: 3.9 Arrangement of wood members for top frame.

Table 3.11 Data for Members of the Hexagons(Figure 3.8)

Member	Type	Quantity (For 5 Hexagons)
B1	A	6
B2	B	30
B3	B	18
B4	B	18
B5	B	18

Table 3.12 Hub Sizes for the Hexagons (Figure 3.8)

Hub	Quantity
A4	6
A3	6
A7	12

Table: 3.13 Member sizes for top structure (Figure 3.9)

Member	Type	Quantity
A2	B	5

Figure 3.10 shows dimension of the members as given in the above tables.

3.6 Structure

Referring to figure 3.11 the structure consists of two circular strips made up of hexagons pentagons and a top frame, which were assembled as explained below.

First Strip: Five pentagons and five hexagons were assembled alternately using nuts, bolts and hubs.

Second Strip: Five hexagons were attached to the top of the first strip.

Top Frame: Top of the hexagons from the second layer was joined with the five corner top frame.

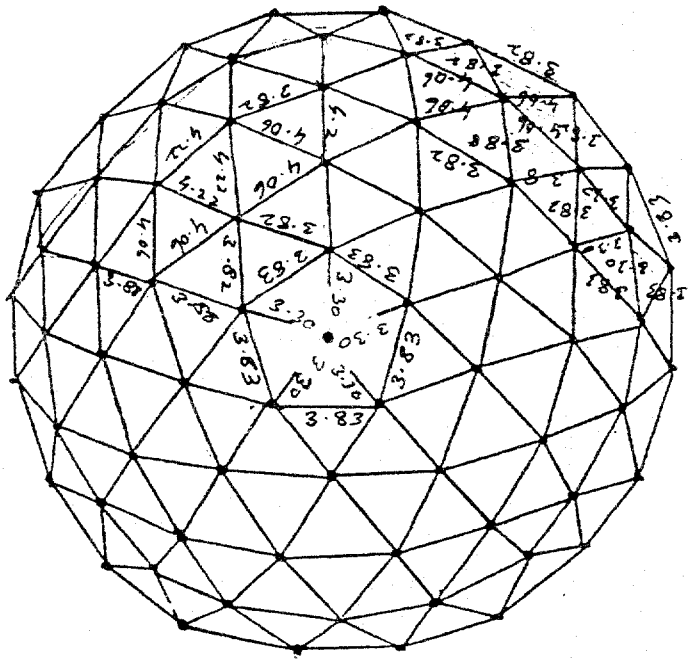

Fig: 3.10 Top view shows dimensions of members.

Second Strip

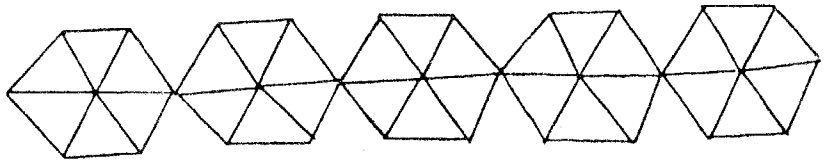

First strip

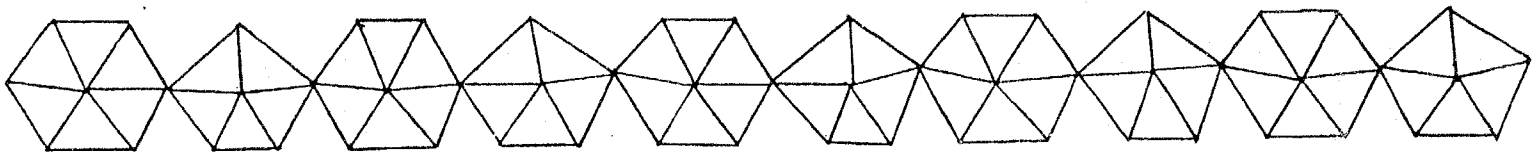

Fig: 3.11 Shows two circular strips used in dome struture.

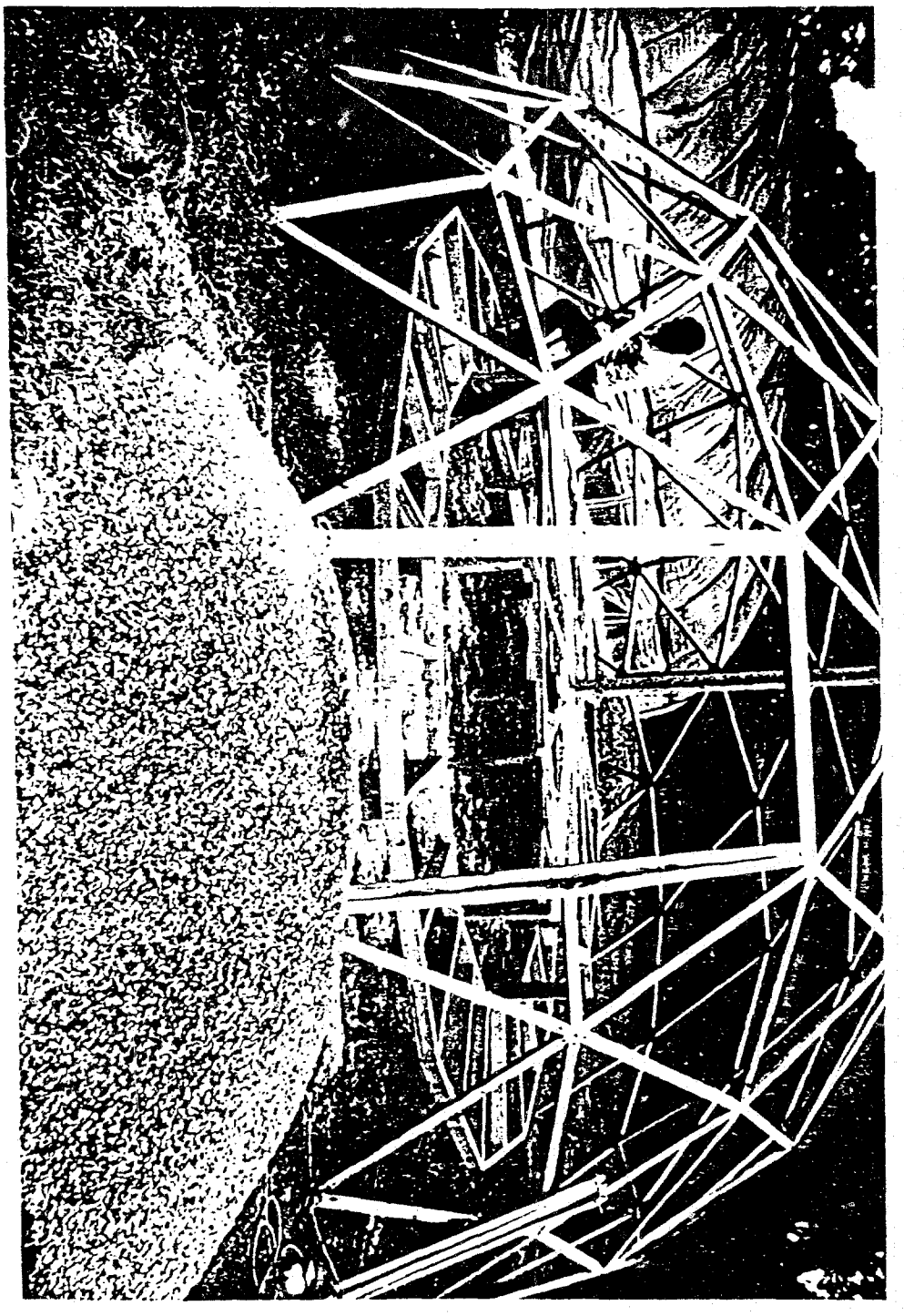

Fig: 3.12 Shows outside frame of geodesic dome.

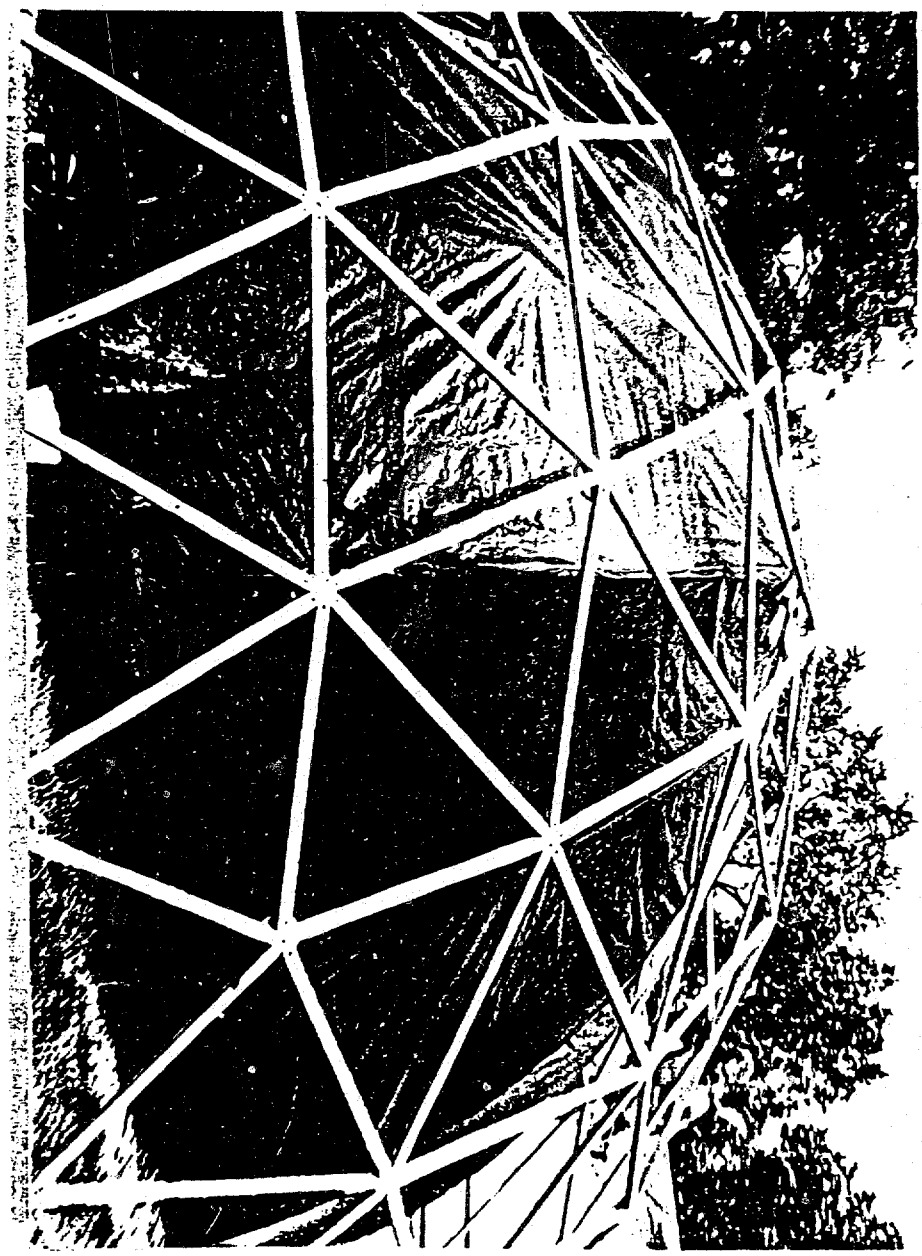

Fig: 3.13 Shows outside frame and inside frame with black plastic.

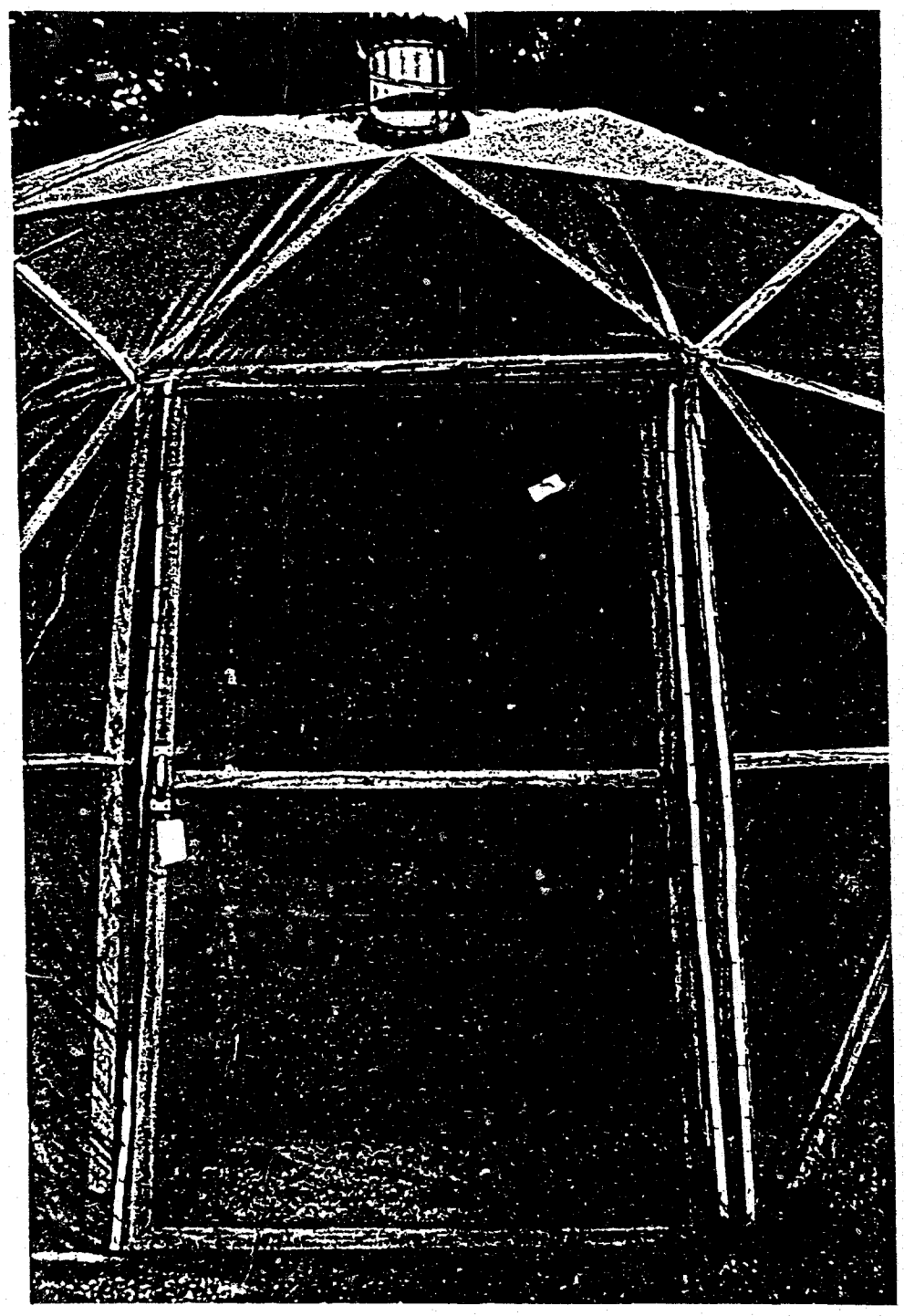

Fig: 3.14 Shows complete arrangement of Natural Air Flow Configuration.

CHAPTER 4
INSTRUMENTATION AND PROCEDURE

A Disk Data Acquisition System(DDAS) as shown in figure 4.1, was used to acquire temperature and relative humidity data at various locations and under varying solar radiation levels at the experimental site. The location of the sensors is shown in Figure 4.2. A wooden box was installed outside the greenhouse for DDAS system equipment and accessories. A PVC pipe was used to run the wires from DDAS to greenhouse.

The DDAS system includes an IBM compatible portable computer with 512 K memory and one 3 1/2" disk drive,one sam 8.12.4 Data Aquisition Module, RS-232 data cable, Ni-Cad batteries, a charger, a powerline filter, a surge suppressor and "dlogger. Bas" data logging software. The Ni-Cad batteries that can run the system for a few hours when fully charged. The system can also be run continuously with the charger plugged into 110 Vac.

Five sensors were used for temperature and two for relative humidity measurements. For humidity measurements "Two-Wire Humidity and Temperature Transmitters" were used with following characterstic.

Measuring Range	0 - 100% RH
Accuracy at +20 C	+2% to -2% RH(0- 90% RH)
	+3% to -3% RH(90-100% RH)
Temperature Coefficient	- 0.04% RH / C
Sensor	- HUMICAP 1638 HM

Velocity was measured by "DATA METRICS" 100 VT Air flow Meter.

PROCEDURE

Solar dryer was tested for drying grapes and the performance was evaluated. The dryer is built out of 4 feet long(1.25"x 2.00") wooden members. It is covered by a transparent tedlar plastic(outer shell) and a black absorber (inner shell). These two shells creat an air space

about two feet wide. This dryer was tested for two different arrangements with fan and without fan, as shown in figures 4.3a and 4.3b. In the first case a fan was used to push the air into the space between two shells and in the second case natural convection was used for suction of the outside air, and a ventilator was used at the exhaust to help increase the airflow. Two trays were filled with grapes. The rest of the trays were covered with a plastic sheet so that all of the heated air went up through the two trays. Fresh grapes were loaded after sunset time, and were weighed every morning (at sun rise time) and every evening at sunset to check the weight loss due to evaporation of moisture. Fan was turned on during the day time only (For the first arrangement). Five thermocouples were used to record temperature of the air at different locations as shown in figure 4.2. Relative Humidity of the air at the inlet and the outlet and solar radiation were also recorded.

Velocity at the outlet(top of the dome) was measured and average air velocity was calculated to find the mass flow rate. From the measurements of the relative humidity, the temperatures and the air flow rate, increase in the moisture content of the air between the inlet and the exit was calculated by use of a computer program given in the appendix.B

1. Power Line
2. Power Supply
3. Power Jumper
4. Power
5. computer ON/OFF
6. Computer
7. RS-232
8. Power
9. Sam
10. Sensors

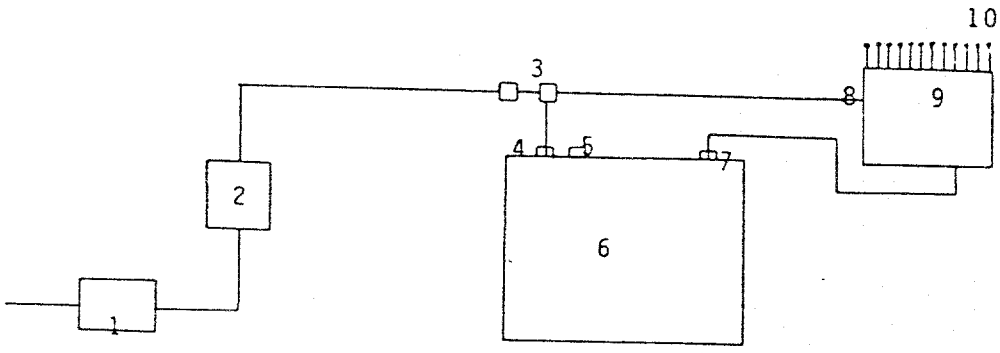

Fig: 4.1 Portable Data Acquisition System.

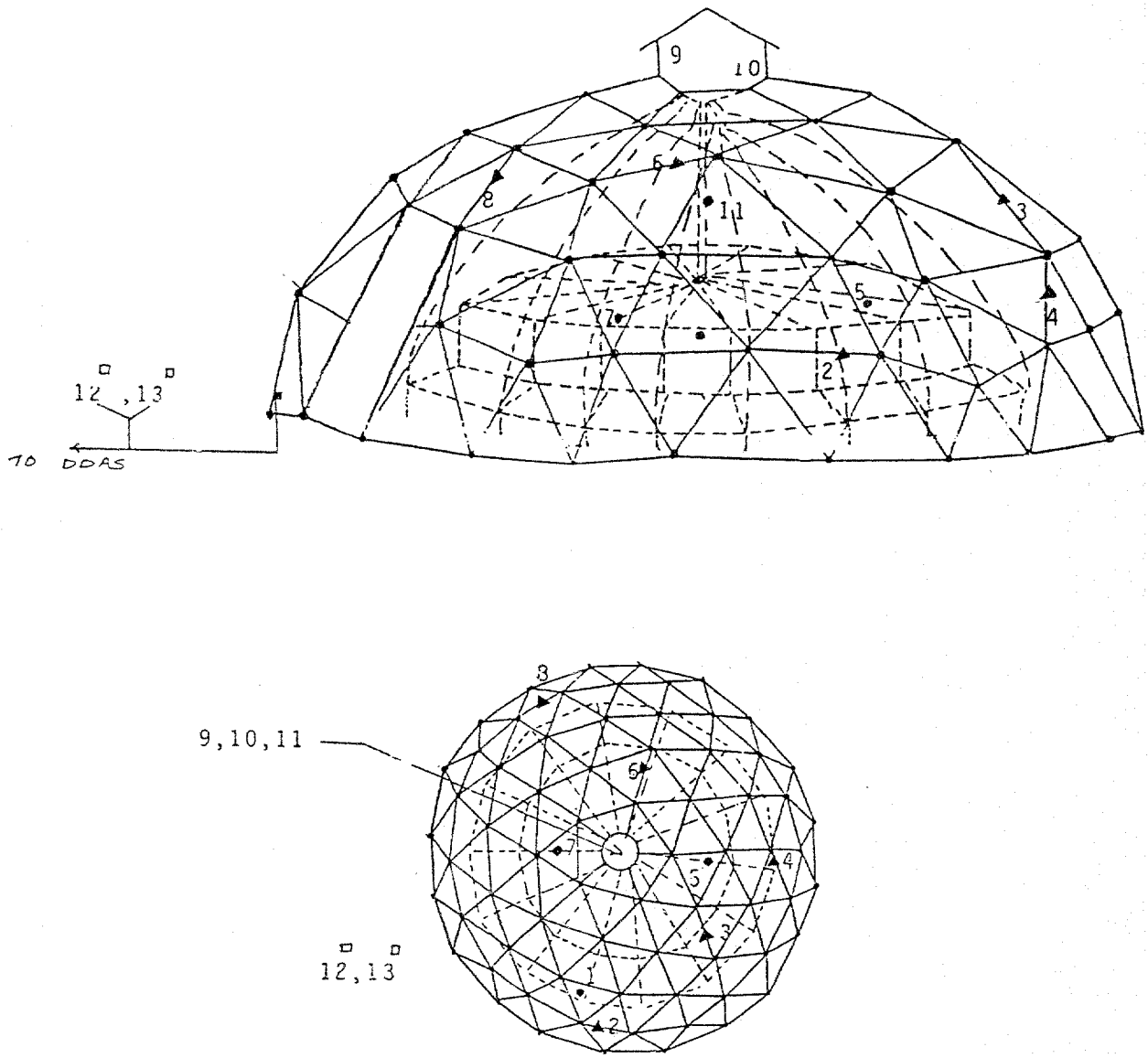

▲ Sensors on inside surface of outer shell
● Location of sensors inside the black Plastic.
Temperature Sensors(1,2,3,4,5,6,7,8,10,12)
Relative Humidity sensors(9,13)

Fig: 4.2 Location of Sensors.

A. Inlet Fan.
B. Exhaust Pipe.
C. Fruit Trays.

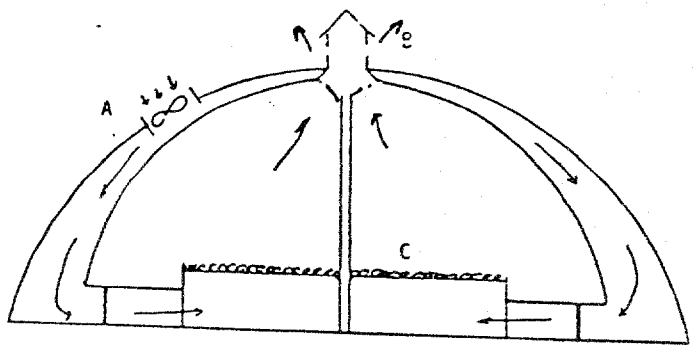

Fig: 4.3a Shows arrangement of Forced Air Configuration.

D. Exhaust Ventilator.
E. 16" Dia Flexible Duct.
F. Fruit Trays.

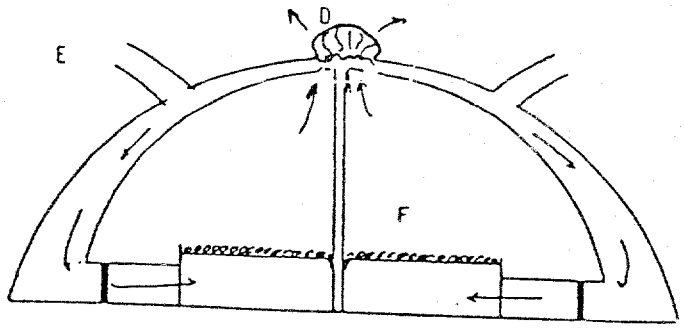

Fig: 4.3b Shows arrangement of Natural Air Flow Configuration.

Chapter 5
Thermal simulation of the solar fruit dryer

Temperature response of the solar dryer under unsteady outside conditions can be studied by simulation using thermal-electrical system analogies. Electrical systems are analogous to many other systems including thermal, mechanical and hydraulic systems. Thermal circuit principle and dynamic system analogies have been applied very successfully to study the rate of heat flow through walls and roof subjected to steady periodic variations in the weather elements. The method is based on the fundamental similarity between the flow of heat within a rigid body and that in a noninductive electric circuit. The analysis is based directly on the identity of the equation governing transient heat flow and the flow of electricity in resistance capacitance circuit.

Princeton Circuit Analysis (PCAP) which is a modified and improved version of Electronic Circuit Analysis Program (ECAP) has been used in this study to obtain the thermal response and the inside air temperature of the solar fruit dryer. The whole model is considered as a solid mass with the temperature changing with time and location as a result of heat exchange with the surrounding.

All lumped properties (k, h, C_p, ρ) are considered to be constant over the temperature range encountered and the space temperature is considered uniform at any instant. In order to simplify the steady-state heat transfer analysis for solar heating of the air, heat capacity of the structure elements and conductive heat losses through the floor to the ground are neglected. In drawing the thermal circuit for the solar dryer, the system components are idealized and represented by circuit elements. The thermal circuit representing the solar dryer is shown in figure 5.1. The heat transfer system represented by the circuit is composed of discrete elements or lumps. Table 5.1 shows the analogies in theraml and electrical systems

Table 5.1. Comparision of Thermal and Electrical Systems

Thermal System	Electrical System
Temperature, T	Voltage
Heat flow, Q	Current
Thermal capacity, C	Capacitance
Thermal conductivity, k	Conductance
Thermal resistance	Resistance

Analogous variables of different physical systems can be interrelated quantitatively. Inter conversion of corresponding thermal and electrical quantities can be obtained by defining a scale factor as:

$$\text{Scale Factor} = \frac{\text{Magnitude of quantity unit in electrical circuit}}{\text{Magnitude of quantity unit in thermal circuit}}$$

The Scale factors used to convert the thermal units into the corresponding electrical units are tabulated in table 5.2.

Table 5.2. Scale Factors for Thermal and Electrical Units

Quantity	Thermal System	Electrical System	Scale factor
Potential	Temperature (^{0} K)	Voltage(volt)	1
Energy flow	Heat flow (W)	Current (amp)	1.27×10^{-7}
Resistance	Thermal resistance (^{0}K/W)	Resistance (ohm)	8×10^{6}
Capacity	Thermal Capacity ($J/^0K$)	Capacitance (farad)	1.25×10^{-7}

The circuit element in figure 5.1 consists of basically three parts:

1. Parallel lumped R-C networks representing thermal conduction path through the structural elements.

2. A resistance network representing radiation exchange between all interior surfaces.

3. Temperature sources connected through appropriate thermal resistance to the network and heat source at various points in the network representing boundary conditions.

The calculation procedures in the analysis are summarized and illustrated by the following steps:

Thermal capacitance:

Thermal capacitance is calculated from the following relation

$$C_t = C_p \rho \, V \qquad (J/^0C) \tag{5.1}$$

$$C = C_t \times 1.25 \times 10^{-7} \qquad \text{(farad)} \tag{5.2}$$

Thermal convection coefficient:

Convection coefficient is defined by 1/h A, where h is obtained considering the wind velocity.

Outside convective coefficient

$$R_{co} = \frac{1}{h_{co} A} \times 8 \times 10^{6} \quad \text{(ohm)} \qquad (5.3)$$

Inside convective coefficient

$$R_{ci} = \frac{1}{h_{ci} A} \times 8 \times 10^{6} \quad \text{(ohm)} \qquad (5.4)$$

Radiation exchange network accounting for direct radiation of the collector and the radiation between surfaces within the solar collector was calculated using the relation:

$$R_{ri} = \frac{1 - \varepsilon}{4 A \varepsilon s T_{av}^{3}} \times 8 \times 10^{6} \quad \text{(ohm)} \qquad (5.5)$$

The value of surface emissivity used in the calculations was 0.95 and the Stefan-Boltzman constant was 5.569×10^{-8} $J/K^4 m^2 s$. A direct radiation resistance and equivalent electric resistances between the internal members were calculated using following relation:

$$R_{sh} = \frac{1}{4 A_h F_{in} \sigma T_{av}^{3}} \times 8 \times 10^{6} \quad \text{(ohm)} \qquad (5.6)$$

Calculated values of the resistances and the capacitances are shown in table 5.3.

Table 5.3. Calculated Values of Resistances and Capacitances

R_s = 0.85 ohm	$R_h = 1.253 \times 10^{4}$ ohm
R_g = ...ohm	$(R_{ri})_s$ = 776.87 ohm
R_{sh} = 23099.39 ohm	$(R_{ri})_h$ = 1186 ohm
R_{sg} = 40887.84 ohm	$(R_{ri})_g$ = 2067.267 ohm
$R_{hg} = 1.14 \times 10^{5}$ ohm	C_a = 10.29 farad
$C_s = 1.98 \times 10^{-3}$ farad	$C_h = 3.85 \times 10^{-3}$ farad
$C_g = 1.7991 \times 10^{-3}$ farad	

The solar heat input (Q) absorbed by various surfaces (absorber and ground) was calculated using coefficient of transparency as 0.75 and absorptivity of the black sheet as 0.95.

Current $I = Q \times 1.25 \times 10^{-7}$ (ampere) (5.7)

Figure 5.2 shows the measured air temperature and the computed air temperature inside the solar house. Coefficient of heat transfer was estimated (ref) considering the air leakage of the air leaving the exhaust pipe. During our experiments flow rate of the air before entering the tray was measured and compared with the capacity of the fan to incorporate the air leakage in calculating convective heat transfer coefficient. Two curves are in very good agrement with each other. By computing the air temperature we can design and calculate the efficiency of the solar fruit dryer.

Nomenclature (Used in this chapter):

Symbols	Subscripts
A = area (m^2)	a = air
C = thermal capacitance ($J/^oC$)	ci = inside convection
C = specific heat ($Kj/Kg\ ^oC$)	co = outside convection
V = volume (m^3)	g = ground
h = coefficient of convective heat transfer ($Kj/m\ hr\ ^ok$)	h = black absorber sheet
I = current (ampere)	ri = radiation resistance
K = thermal conductivity ($Kj/hr\ m^oK$)	s = transparent sheet
Q = heat flow (Kj/hr)	t = thermal unit
R = resistance	

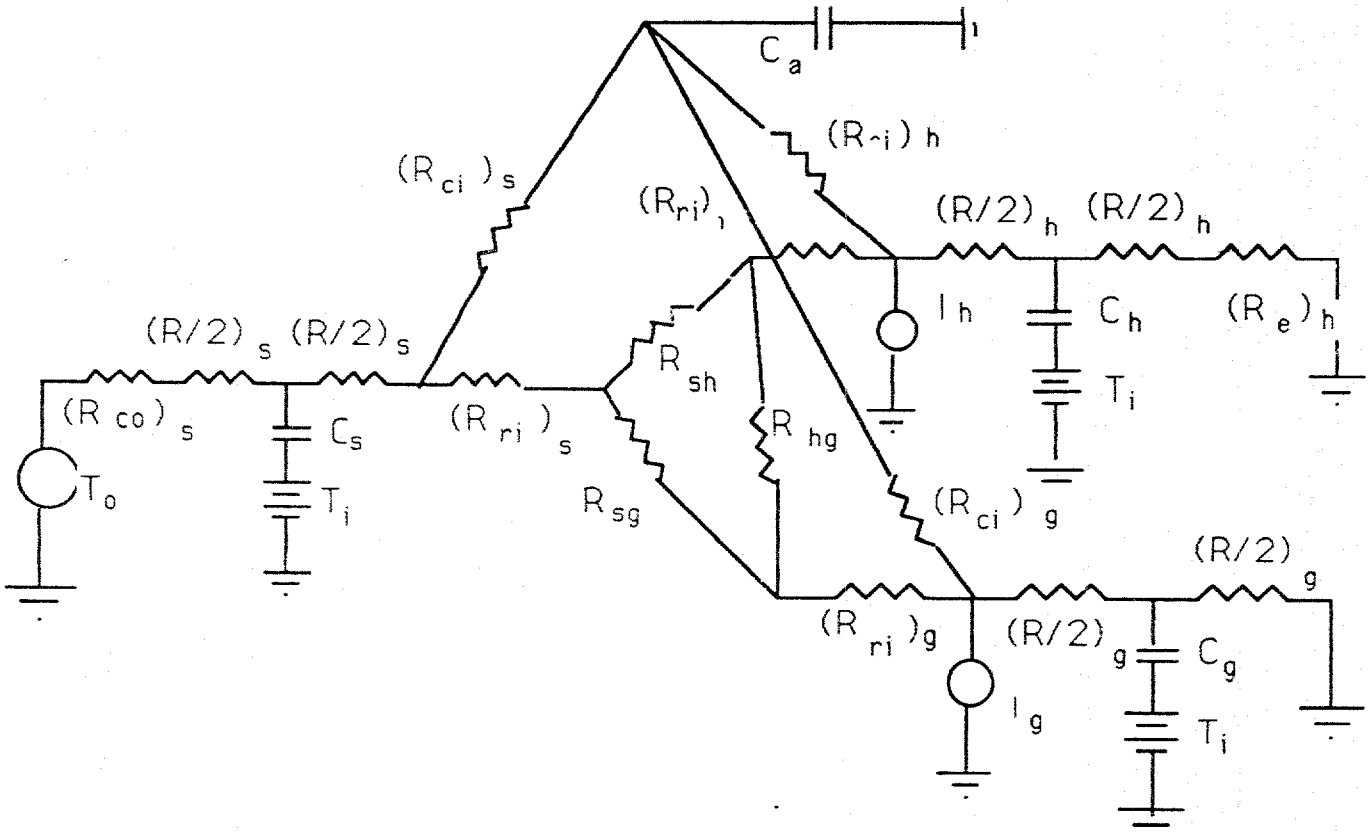

Fig.5.1 Thermal circuit simulation model

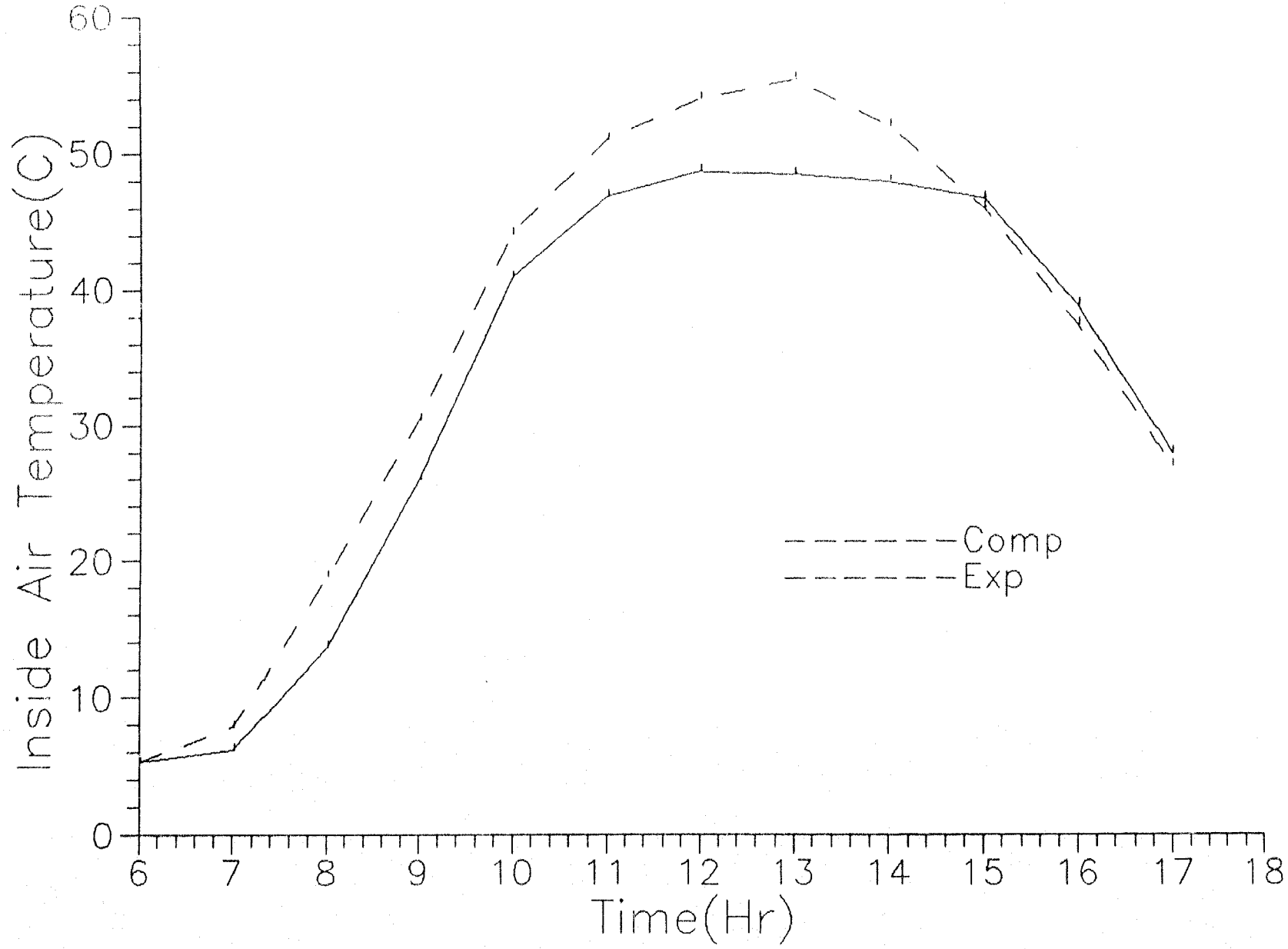

Fig: 5.2 Inside air temperature

CHAPTER 6
RESULTS

This section describes the results of the experiments conducted to find out the performance of the solar dryer. First, three sets of data were recorded with the fan turned on, as shown in figure 4.3.a then the set up was changed as shown in figure 4.3.b.

Experiment No:1

Table 6.1 Shows the weight data for 15 days including 4 cloudy days, that shows the amount of moisture removed from the grapes during this period.

Complete data for the inside and outside ambient temperatures, and the moisture loss from the grapes was recorded every 12 hours and plotted with respect to time as shown in figures 6.1 and 6.2.

TABLE 6.1 Measured Weight of Grapes for the Forced Air Configuration

Date	Time	Wt(kg)	% Moisture Reduction	Remarks
Ø1-27-89	4:5Ø pm	7.82		Sunny
Ø1-28-89	7:ØØ am	7.55	3.45	Sunny
	6:ØØ pm	7.2	8.Ø8	
Ø1-29-89	7:Ø5 am	7.1	9.46	Sunny
	6:15 pm	6.9	12.27	
Ø1-3Ø-89	7:1Ø am	6.7	15.16	Sunny

Table 6.1 (cont'd)

Ø1-3Ø-89	3:Ø5 pm	6.5	18.14	
Ø1-31-89	7:15 am	6.45	18.91	Sunny
	5:3Ø pm	6.21	22.63	
Ø2-Ø1-89	7:1Ø am	6.1	24.43	Sunny
	5:ØØ pm	5.85	28.53	
Ø2-Ø2-89	7:15 am	5.75	3Ø.23	Sunny
	5:ØØ pm	5.5Ø	34.57	
Ø2-Ø3-89	7:2Ø am	5.35	37.37	Sunny
	5:15 pm	5.12	41.67	
Ø2-Ø4-89	1:3Ø pm*	5.ØØ	43.97	Cloudy
Ø2-Ø6-89	9:3Ø am*	4.75	48.97	Cloudy
Ø2-Ø7-89	6:3Ø pm	4.6Ø	52.12	Cloudy
Ø2-Ø8-89	2:35 pm	4.49	54.52	Sunny
Ø2-Ø9-89	5:3Ø pm	4.3Ø	58.57	Sunny
Ø2-1Ø-89	4:3Ø pm	4.1Ø	63.4	Sunny

* Rain Period

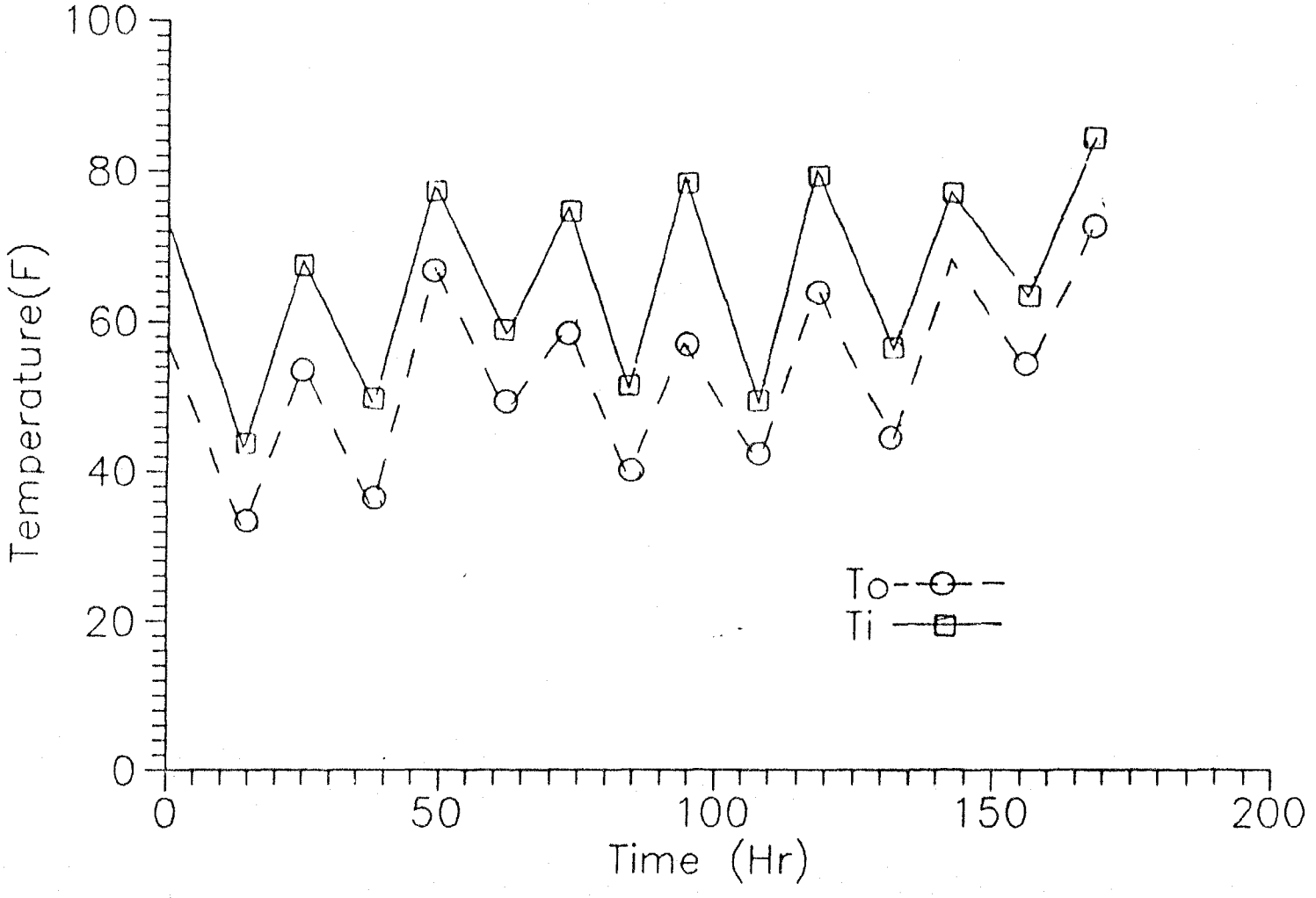

Fig: 6.1 Measured value of Temperature in solar dryer.
(Forced Air Configuration)

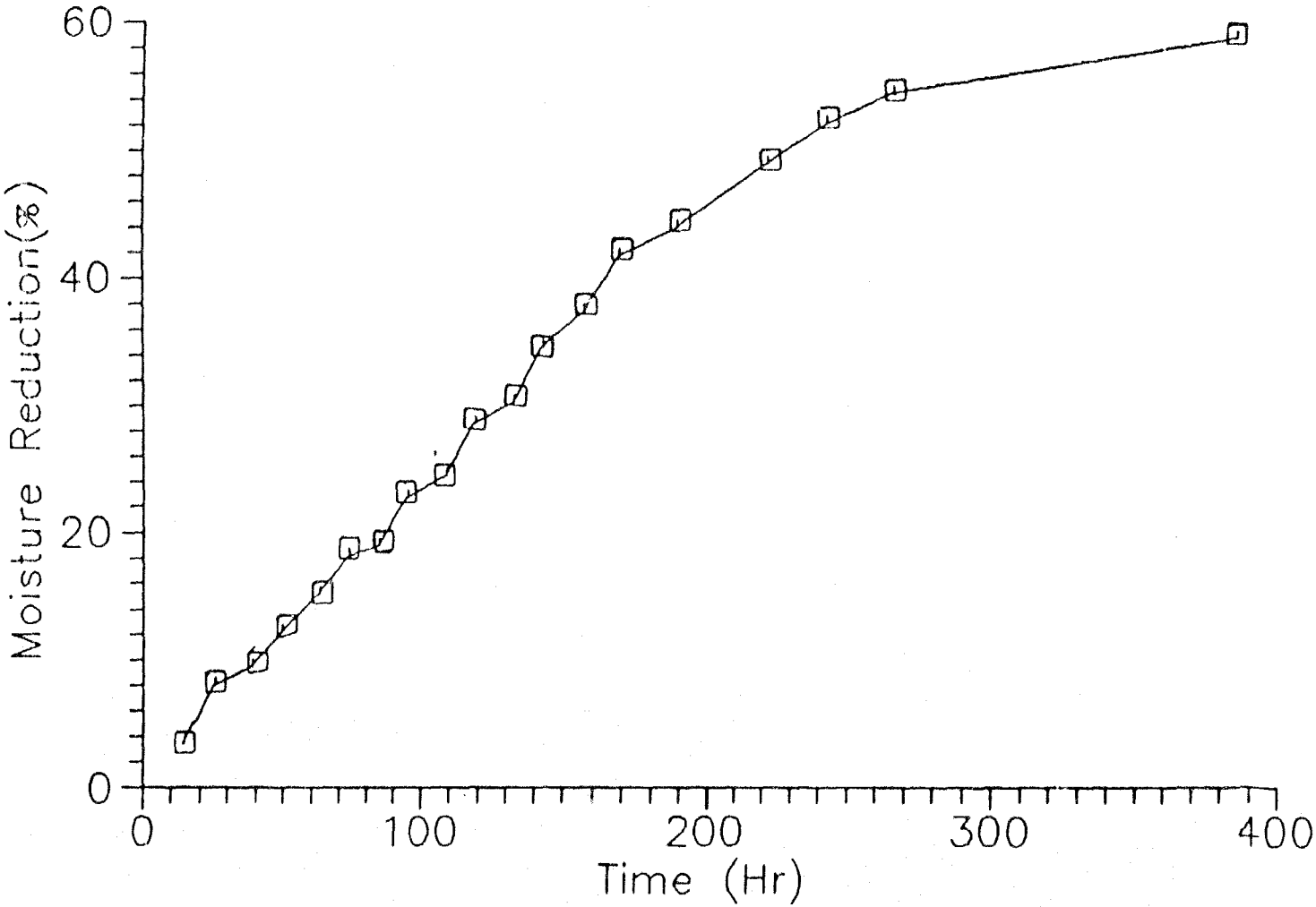

Fig: 6.2 Moisture Reduction(%) vs Time.
(Forced Air Configuration)

Experiment No: 2

In this experiment grapes were loaded for fourteen days, in which three days were cloudy and rest of the days were sunny. Table 6.2 and figures 6.3 to 6.5 give the results of the experiment.

Table: 6.2 Measured Weight of Grapes for the Forced Air Configuration.

Date	Time	Wt(kg)	% Moisture Reduction	Remarks
Ø3-29-89	6:ØØ pm	6.95		
Ø3-3Ø-89	7:3Ø am	6.6	5.ØØ	Cloudy
	6:15 pm	6.5	6.51	
Ø3-31-89	7:45 am	6.4	8.Ø2	Sunny
	5:5Ø pm	6.1	12.7	
Ø4-Ø1-89	8:ØØ am	6.Ø	14.34	Sunny
	6:ØØ pm	5.7	19.34	
Ø4-Ø2-89	7:ØØ am	5.6	21.Ø5	Sunny
	6:ØØ pm	5.3	26.39	
Ø4-Ø3-89	1Ø:3Ø am	5.2	28.27	Sunny
	5.45 pm	4.95	33.Ø7	
Ø4-Ø4-89*	9:2Ø am	4.85	35.Ø9	Sunny
	5:45 pm	4.6	4Ø.27	
Ø4-Ø9-89*	9:15 am	4.1	51.1	Sunny
	7:3Ø pm	3.95	54.75	
Ø4-11-89	9:45 am	3.85	57.28	Sunny
	7:3Ø pm	3.65	62.47	
Ø4-12-89	8:3Ø am	3.6	63.83	Sunny
	7:3Ø pm	3.4	69.38	
Ø4-13-89	8:3Ø am	3.35	7Ø.85	Sunny

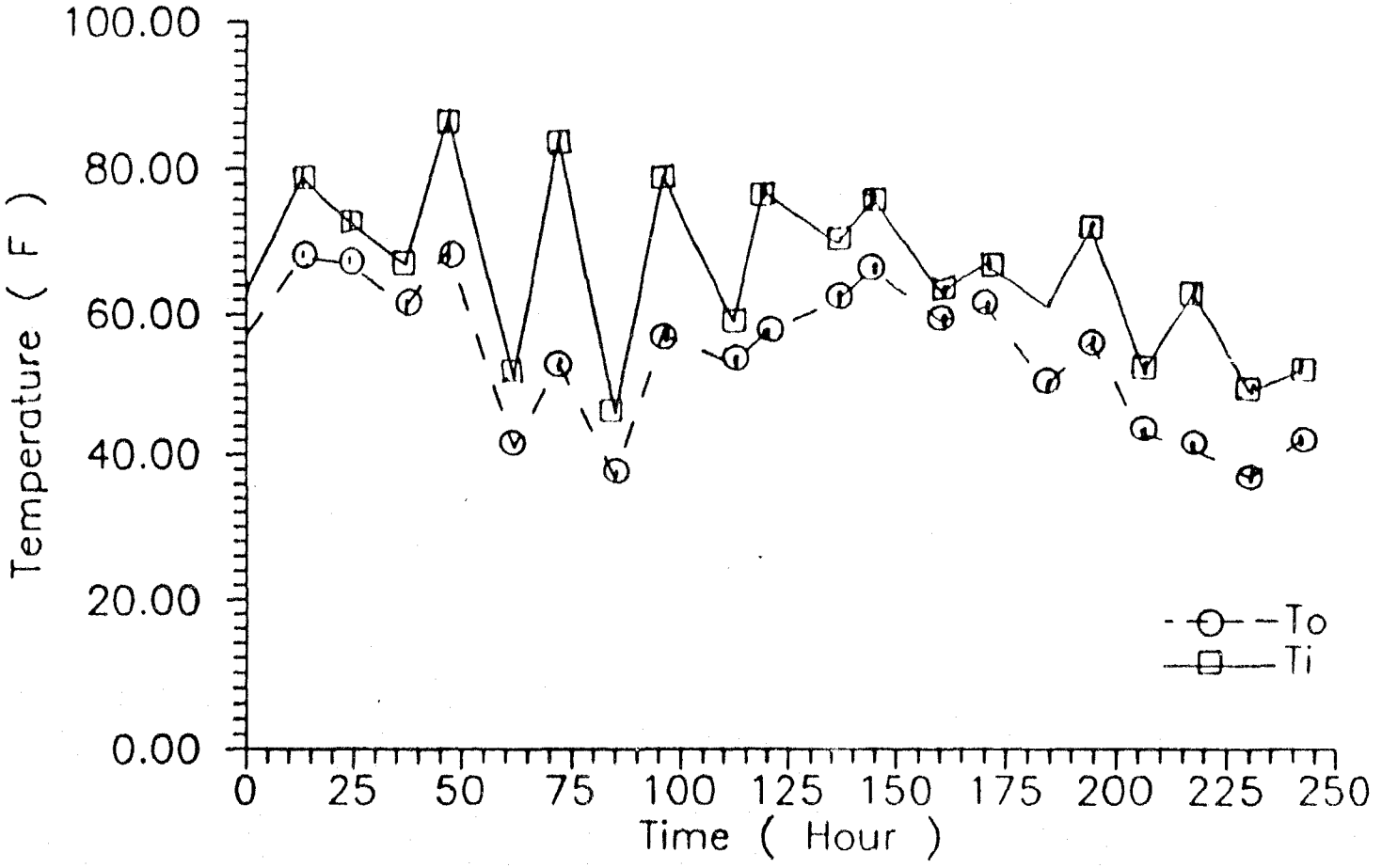

Fig: 6.3 Measured value of Temperature in solar dryer (Forced Air Configuration)

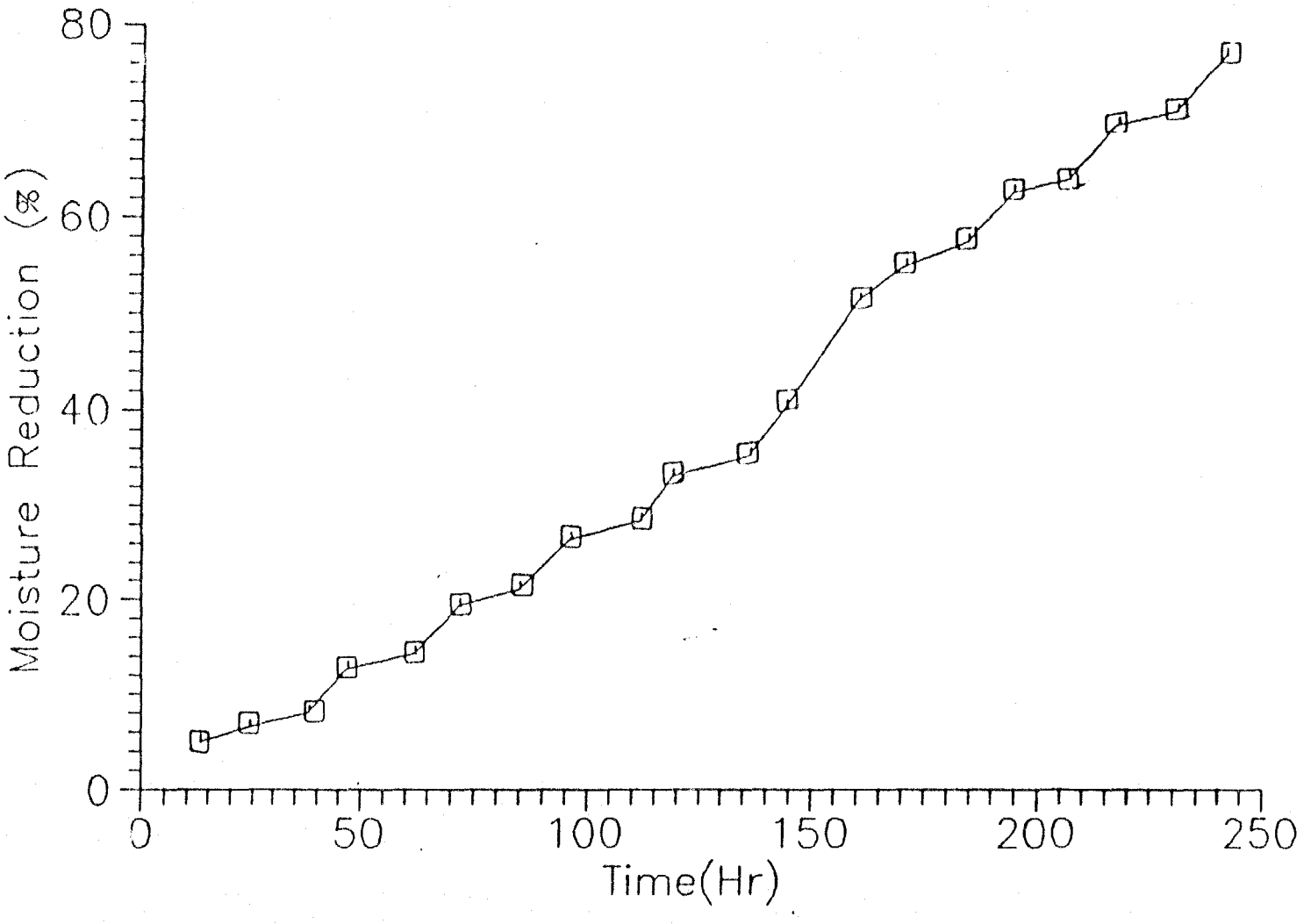

Fig: 6.4 Moisture Reduction (%) vs Time.
(Forced Air Configuration)

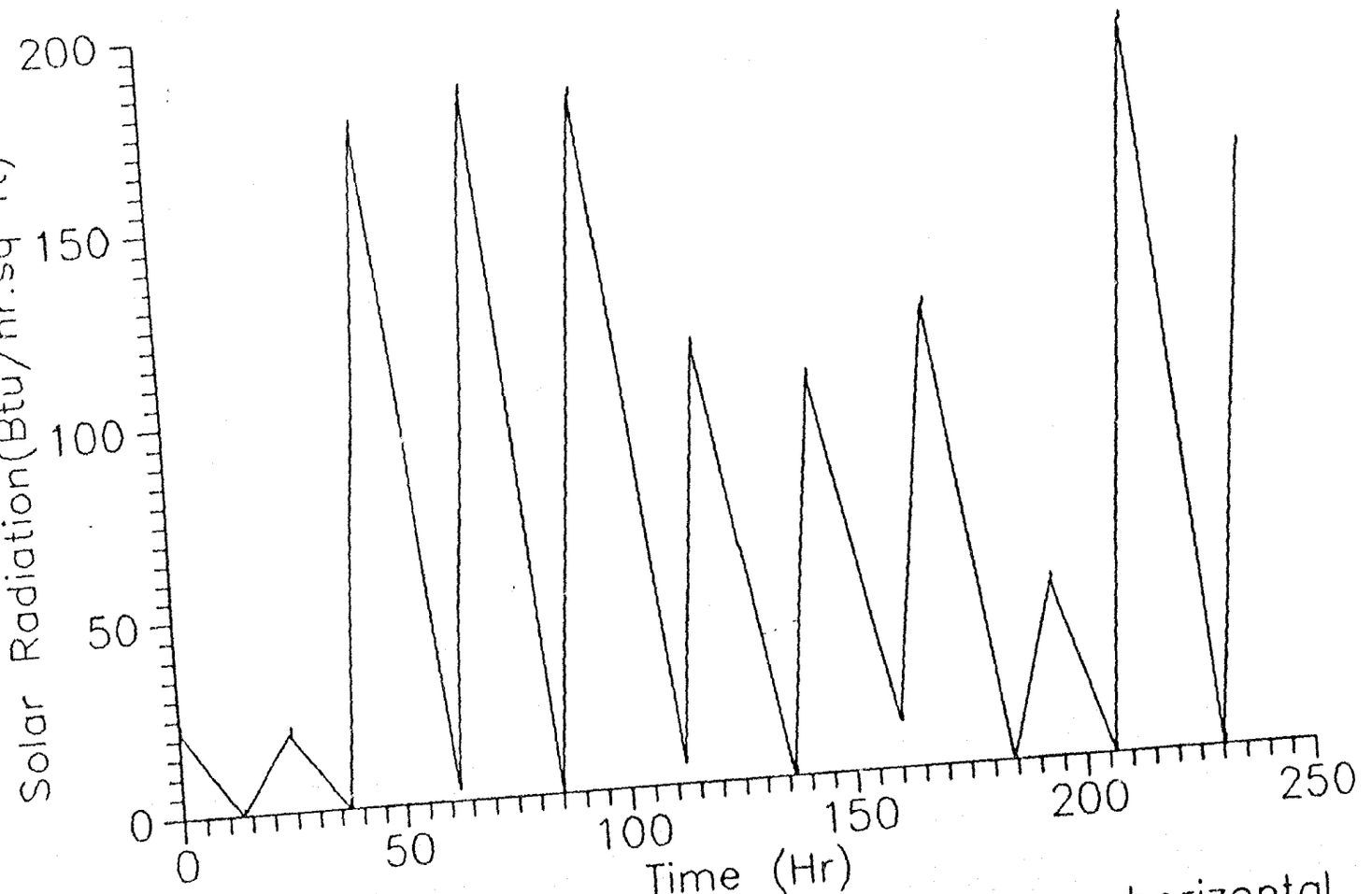

Fig: 6.5 Measured value of Solar Radiation on a horizontal surface outside the solar dryer.
(Forced Air Configuration)

Ø4-13-89	8:3Ø am	3.35	7Ø.85	Sunny	
	7:3Ø pm	3.15	76.8		* Rain Period

Experiment No.3

Data for one day was recorded and analyzed in this experiment. Moisture removed was calculated by two different methods and compared with theoretical simulation results.

In the first method grapes were weighed at sunrise and sunset times, Table 6.3 gives the difference in the weight. In the second method moisture removed was found by humidity and temperature calculations. Table 6.4 shows all the calculations to find the mass flow rate of the moist air.

Volume flow rate and mass flow rate were calculated using the following formulas and the procedure:

$$m = Q.(A-B) \quad (6.1)$$

$$A = Wo/Vo \quad (6.2)$$

$$B = Wi/Vi \quad (6.3)$$

where

m is the mass flow rate of air.
Q is the volumetric flow rate of air
W is the humidity ratio.
V is the specific volume.

Subcript "o" stands for the outgoing
and "i" stands for the incoming air in the dryer.

Humidity Ratio and specific volume are found from a psychometric chart, using the temperature and the relative humidity for each hour. Volume flow rate Q is calculated from the average velocity at the exhaust pipe, which in turn is calculated from the velocity measurements at different points at the exhaust.

Table 6.3 Measured Weight of Grapes for the Forced Air Configuration.

Date	Time	Weight (Kg)	Decrease in Weight (Kg)	Remarks
Ø6-3Ø-89	8:ØØ am	6.9		

4:ØØ pm	6.1	Ø.8	sunny	

Table 6.4 Data for Rate of Moisture Removed Based on the Air Temperature and Humidity Measurements (Forced Air Configuration, Q=154.64 CFM)

Time		V cu.ft/Ibm	W Ibm/Ibd	A=Wo/Vo Ibm/cu ft	B=Wi/Vi Ibm/cu ft	mx6Ø Ib/hr
Ø8:ØØ	O	13.57	Ø.Ø1Ø6	Ø.ØØØ7811		
	I	13.44	Ø.Ø1ØØ		Ø.ØØØ744	Ø.343
Ø9:ØØ	O	13.69	Ø.Ø1Ø4	Ø.ØØØ759		
	I	13.6Ø	Ø.ØØ99		Ø.ØØØ727	Ø.295
1Ø:ØØ	O	13.92	Ø.ØØ95	Ø.ØØØ682		
	I	13.72	Ø.ØØ85		Ø.ØØØ619	Ø.588
11:ØØ	O	14.17	Ø.ØØ97	Ø.ØØØ684		
	I	13.8Ø	Ø.ØØ85		Ø.ØØØ615	Ø.636
12:ØØ	O	14.39	Ø.Ø1Ø8	Ø.ØØØ75Ø		
	I	13.93	Ø.Ø1Ø4		Ø.ØØØ746	Ø.Ø41
13:ØØ	O	14.59	Ø.Ø125	Ø.ØØØ858		
	I	13.95	Ø.Ø111		Ø.ØØØ795	Ø.564
14:ØØ	O	14.7Ø	Ø.Ø14Ø	Ø.ØØØ952		
	I	14.Ø1	Ø.Ø123		Ø.ØØØ878	Ø.673
15:ØØ	O	14.65	Ø.Ø135	Ø.ØØØ921		
	I	14.Ø1	Ø.Ø124		Ø.ØØØ885	Ø.337
16:ØØ	O	14.7Ø	Ø.Ø135	Ø.ØØØ918		
	I	14.Ø5	Ø.Ø125		Ø.ØØØ889	Ø.266

Moisture removed was also found theoretically, using the following relations [29]:

$$M(e)=[1-rh/c.T]^{1/n} \qquad (6.4)$$

Where rh = equilibrium relative humidity
M(e)= equilibrium moisture content, dry basis
T = temperature, degrees R
c,n = constants
$c = 7.13 \times 10^{-5}$
n = 1.02

$$\{ M(t)-M(e) \} / M(0)-M(e) = A\ e \qquad (6.5)$$

Where M(t)= moisture content,dry basis,after time t.
M(0)= moisture content,dry basis, at time t=0,
A = 8/Pi =0.811
K = Dv. (Pi/2a) (6.6)
Dv = Mass Diffusivity= 5.41×10 sq m/ hour
a = Half thickness

Figures 6.6 and 6.7 show variation of relative humidity, Temperature between the inlet and the outlet. Figure 6.8 shows comparison between theoretical results and the experimental results. The deviation between the theoretical and the experimental results is explained later in this chapter.

Experiment No.4

In this experiment we changed the arrangement of the solar dryer, as shown in figure 4.3.b. In this arrangement the air flow occured by natural convection. Table 6.5 and figures 6.9 to 6.11 give the result of such arrangement.

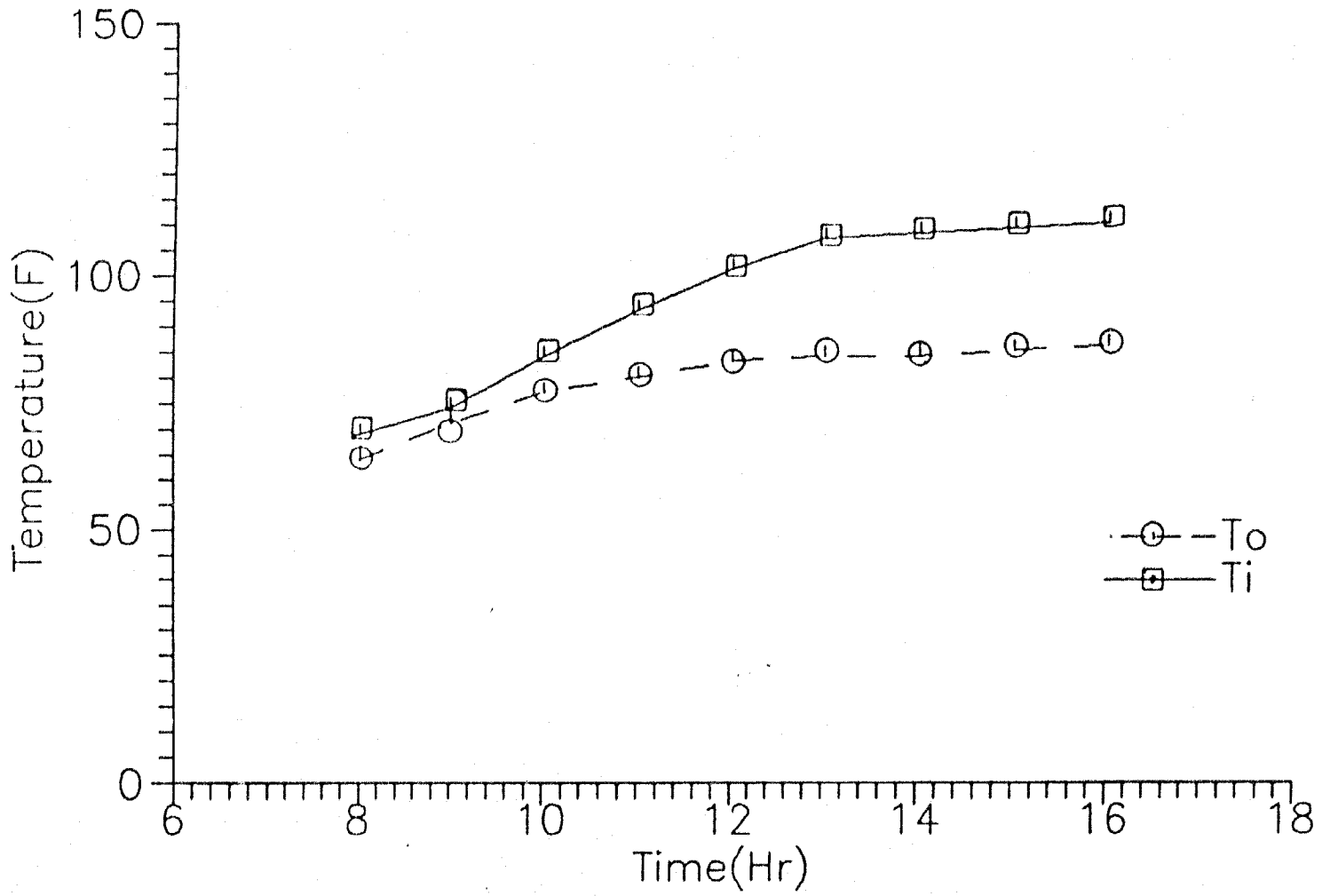

Fig: 6.6 Measured value of Temperature in solar dryer.
(Forced Air Configuration)

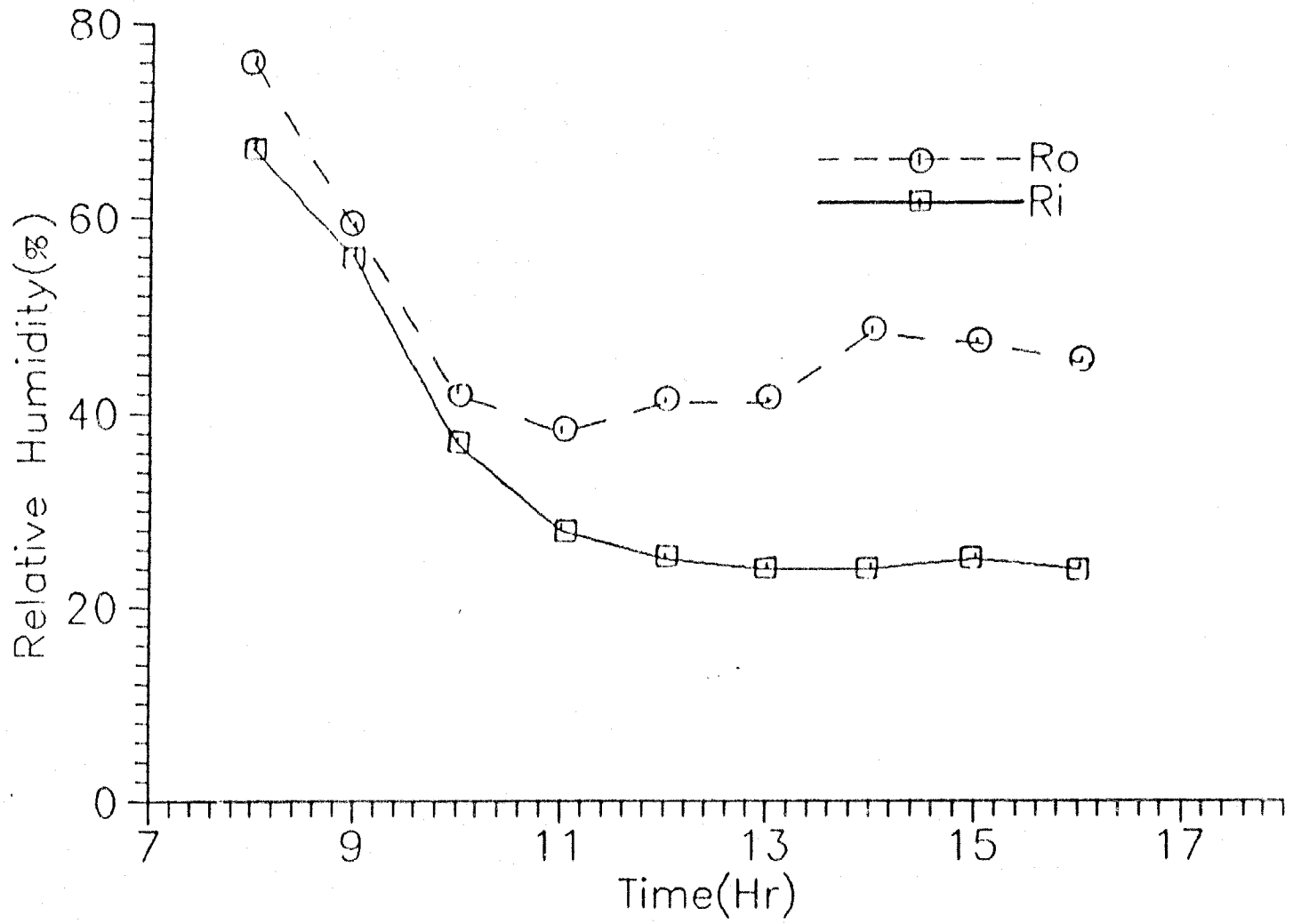

Fig: 6.7 Measured value of Relative Humidity in solar dryer.(Forced Air Configuration)

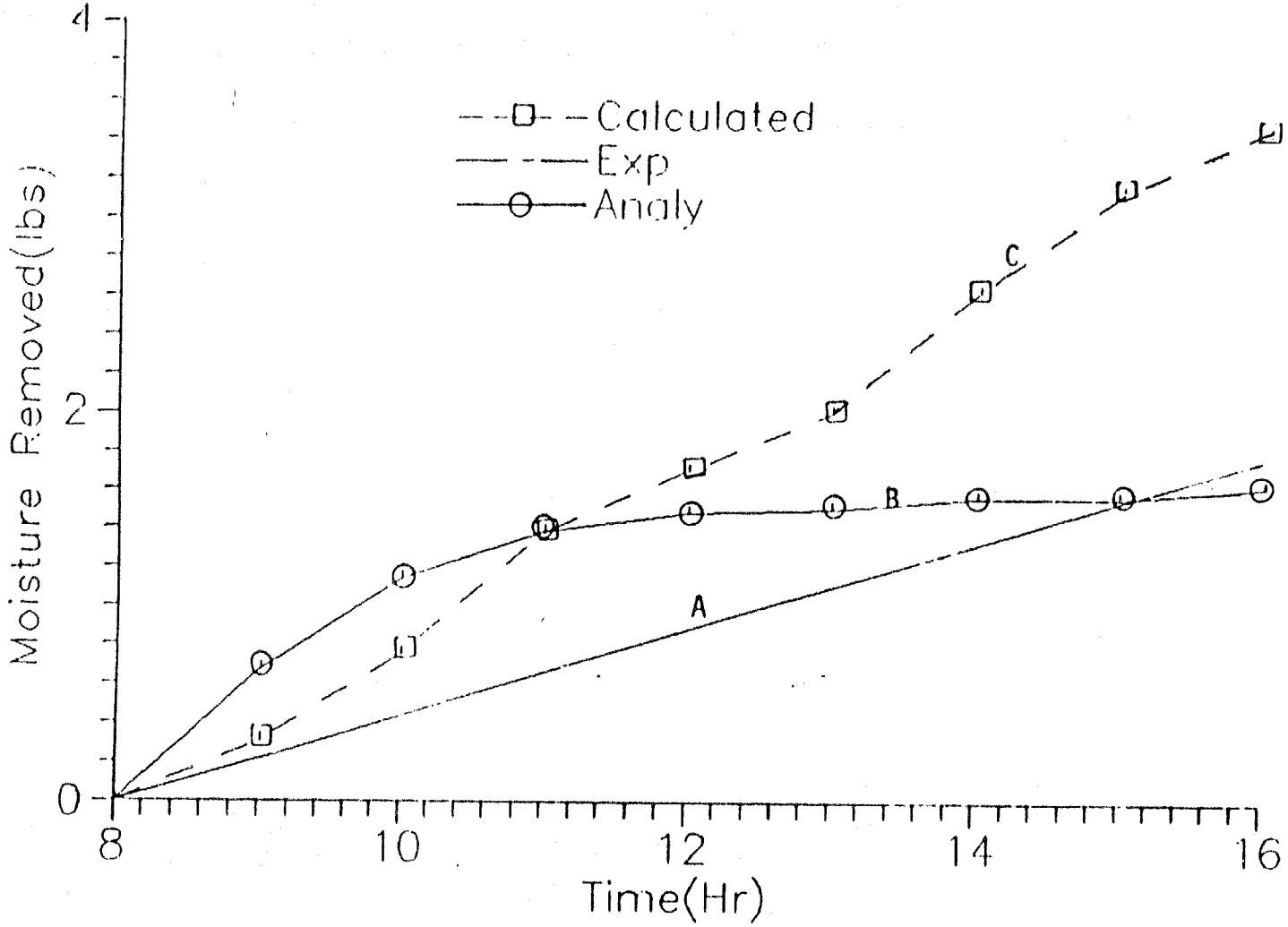

Fig: 6.8 Cumulative amount of moisture removed with respect to time(Analytical & Experimental) (Forced Air Configuration)

TABLE 6.5 Measured Weight of Grapes for the Natural Air Flow Conf[illegible]

Date	Time	Wt(kg)	% Moisture Reduction	Remarks
Ø4-29-89	7:45 am	7.4		
	7:3Ø pm	6.9	6.75	Sunny
Ø4-3Ø-89	7:3Ø am	6.8	7.89	
	7:45 pm	6.4	13.77	Sunny
Ø5-Ø1-89	7:25 am	6.3	15.33	
	6:45 pm	5.9	21.23	Sunny
Ø5-Ø2-89	8:ØØ am	5.8	22.95	
	7:3Ø pm	5.4	29.83	Sunny
Ø5-Ø3-89	8:15 am	5.3	31.68	
	7:ØØ pm	5.Ø	37.34	Sunny
Ø5-Ø4-89	8:ØØ am	4.9	39.34	
	7:3Ø pm	4.7	43.42	[illegible]y
Ø5-Ø6-89	7:45 am	4.5	47.67	
	8:Ø4 pm	4.3	52.11	Cloudy
Ø5-Ø7-89	7:3Ø am	4.2	54.34	
	6:58 pm	4.Ø	62.1	Sunny
Ø5-Ø8-89	8:3Ø am	3.9	64.6	
	8:ØØ pm	3.7	69.72	Sunny
Ø5-Ø9-89	7:45 am	3.65	71.Ø7	
	6:55 pm	3.4Ø		Sunny

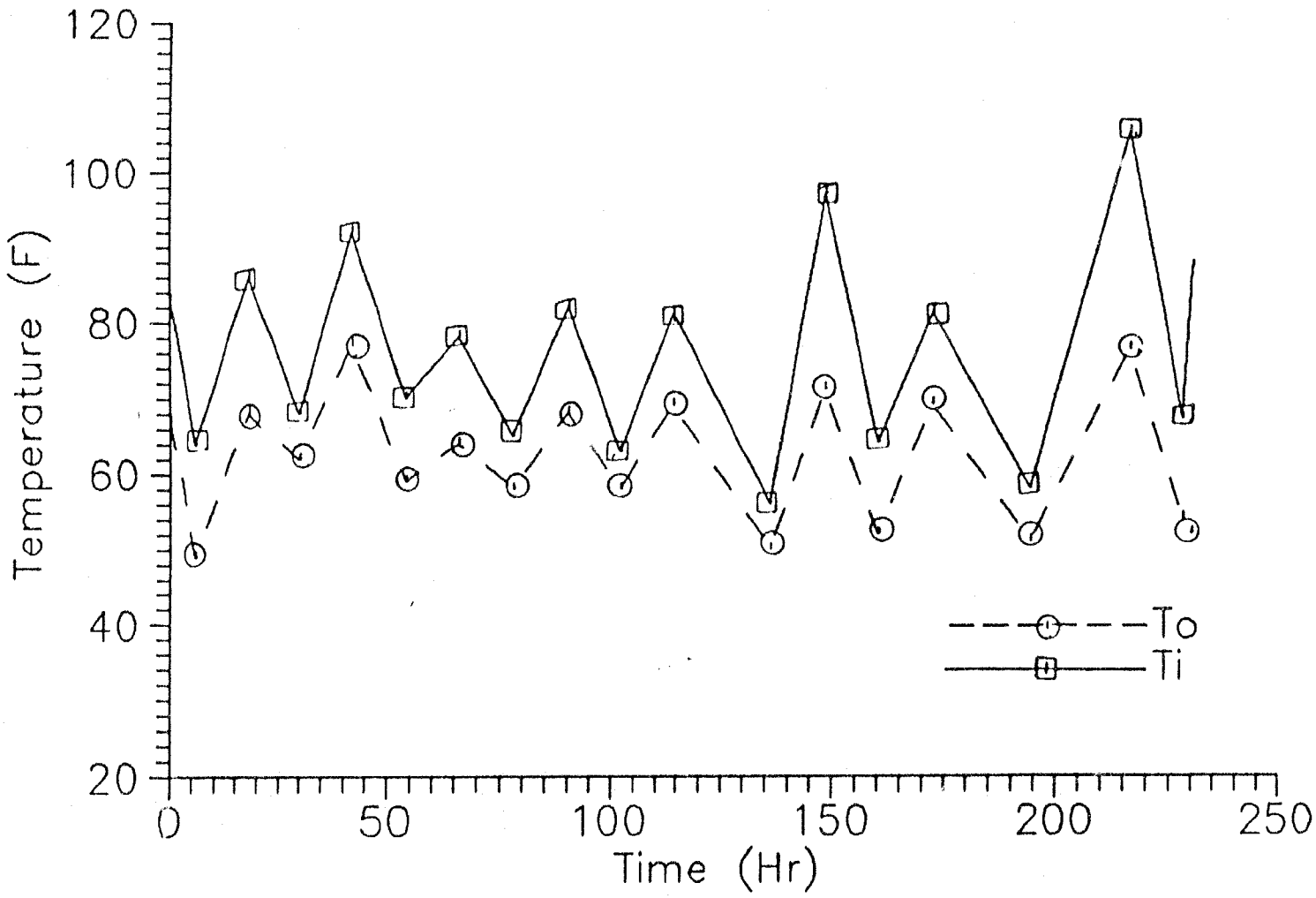

Fig: 6.9 Measured value of Temperature in solar dryer.
(Natural Air Flow Configuration)

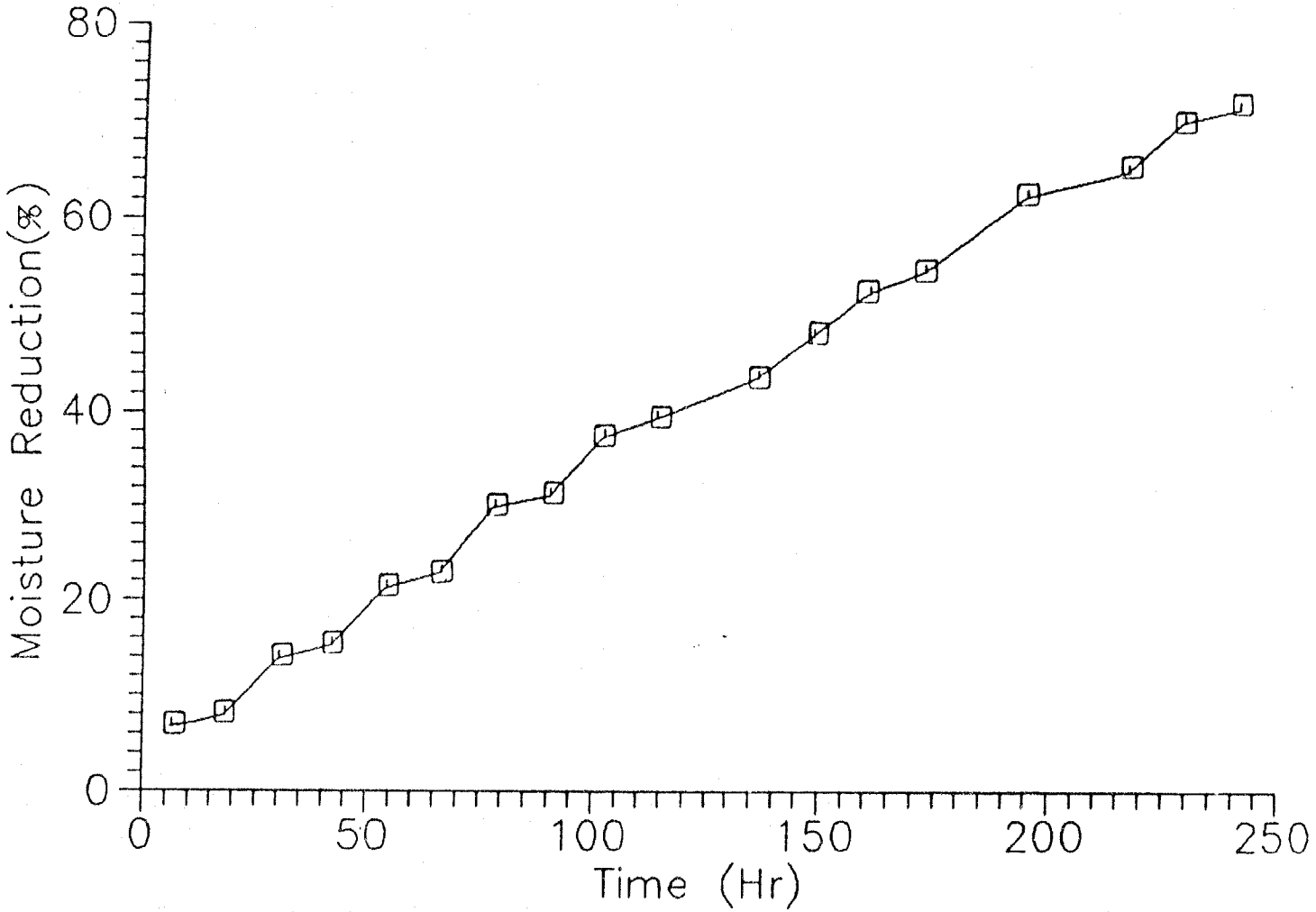

Fig: 5.10 Moisture Reduction (%) vs Time
(Natural Air Flow Configuration)

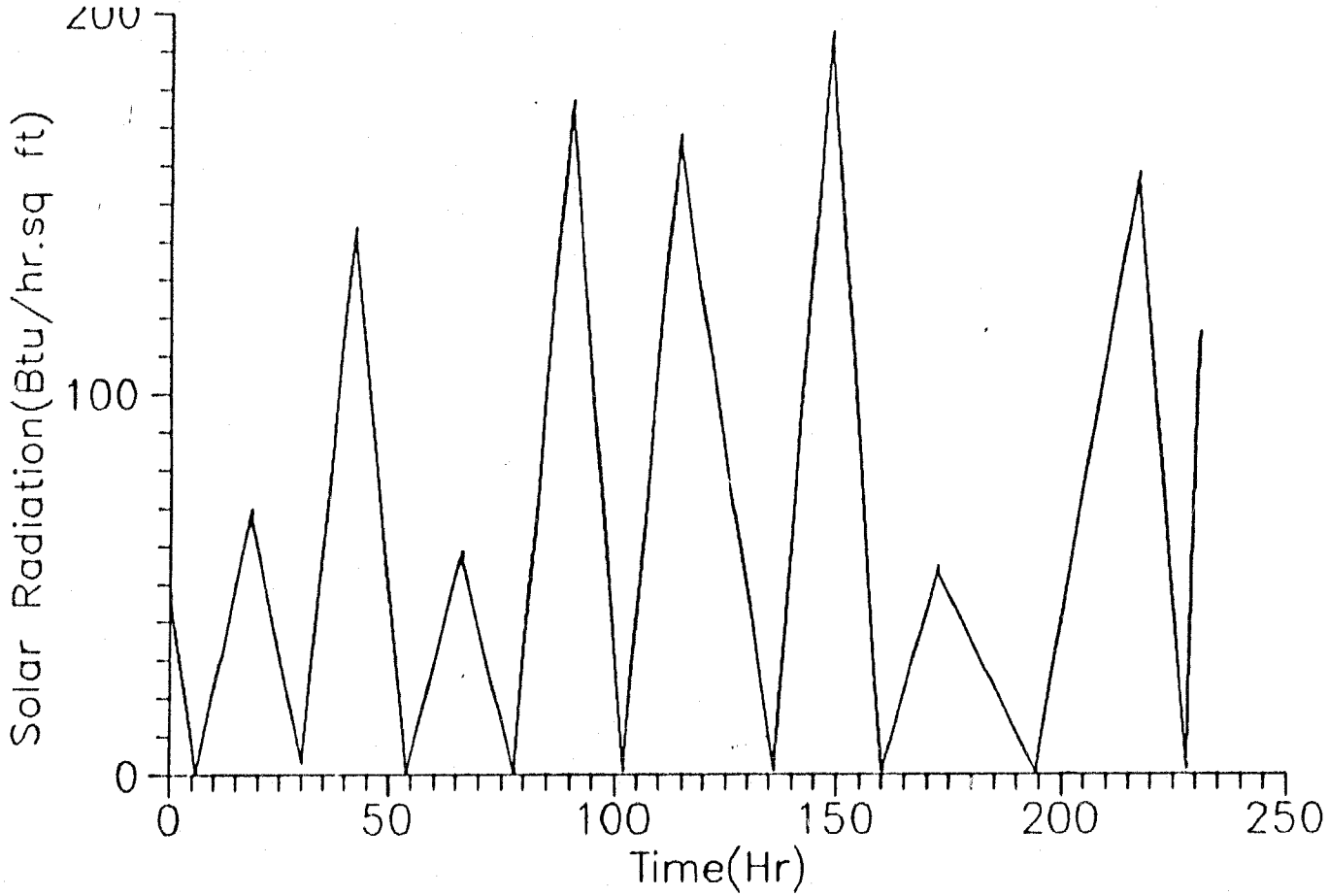

Fig: 6.11 Measured value of Solar Radiation in solar dryer.
(Natural Air Flow Configuration)

Experiment No.5

Data for one day were recorded and analyzed in this experiment with the same arrangement as in Experiment No 4. Moisture removed was calculated by two different methods as discussed earlier and compared with the theoretical simulation results.

Table 6.6 and 6.7 show the data and calculations for both methods respectively and figures 6.12 and 6.13 show the variation of the temperature and the relative humidity for each hour, obtained from theoretical calculations.

Fig 6.14 shows a comparison of the experimentally measured moisture loss with the theoretical simulation results.

TABLE: 6.6. Measured Weight of Grapes for the Natural Air Flow Configuration.

DATE	TIME	WEIGHT	DECREASE in Weight (Kg)	Remarks
Ø6-Ø3-89	7:ØØ am	8.89		
	7:3Ø pm	7.8	1.Ø1	Sunny

TABLE: 6.7 Rate of Moisture Removed Based on the Air Temperature and Humidity Measurements (Natural Air Flow Configuration)

Time		V cu.ft.	W Ib/Ib	A=Wo/Vo Ib/cu ft	B=Wi/Vi Ib/cu ft	m Ib/hr
Ø7:ØØ	I	13.7Ø	Ø.Ø13Ø	9.46×10^{-4}		
	O	13.59	Ø.Ø128		9.41×10^{-4}	Ø.Ø38
Ø8:ØØ	O	13.74	Ø.Ø136	9.8×10^{-4}		
	I	13.61	Ø.Ø116		8.52×10^{-4}	Ø.98Ø

Table 6.7 (cont'd)

09:00	O	13.82	0.0121	8.7×10^{-4}		
	I	14.05	0.0110		7.82×10^{-4}	0.674
10:00	O	13.98	0.0123	8.79×10^{-4}		
	I	13.90	0.0122		8.77×10^{-4}	0.015
11:00	O	14.36	0.0126	8.77×10^{-4}		
	I	14.22	0.0120		8.43×10^{-4}	0.260
12:00	O	14.76	0.0170	11.5×10^{-4}		
	I	14.29	0.0117		8.18×10^{-4}	2.54
13:00	O	15.02	0.0209	13.9×10^{-4}		
	I	14.32	0.0139		9.707×10^{-4}	3.19
14:00	O	14.89	0.0167	11.2×10^{-4}		
	I	14.30	0.0143		10.2×10^{-4}	0.919
15:00	O	15.14	0.0223	14.73×10^{-4}		
	I	14.30	0.0155		10.8×10^{-4}	3.010
16:00	O	15.16	0.0234	15.3×10^{-4}		
	I	14.25	0.0155		10.8×10^{-4}	3.42
17:00	O	14.96	0.0206	13.77×10^{-4}		
	I	14.19	0.0161		11.34×10^{-4}	1.86
18:00	O	14.80	0.0186	12.56×10^{-4}		
	I	14.18	0.0151		10.6×10^{-4}	1.50

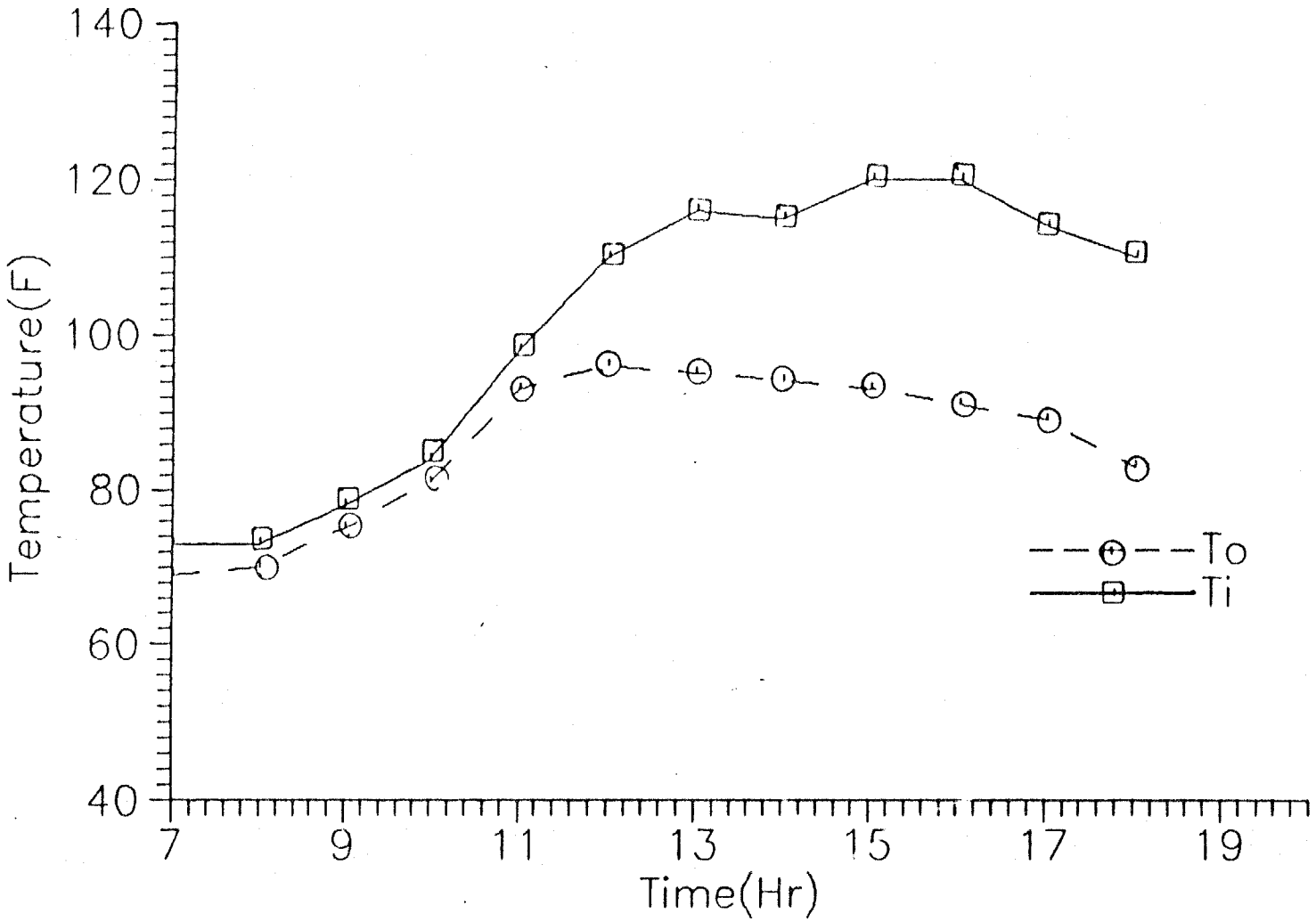

Fig: 5.12 Measured value of Temperature in solar dryer.
(Natural Air Flow Configuration)

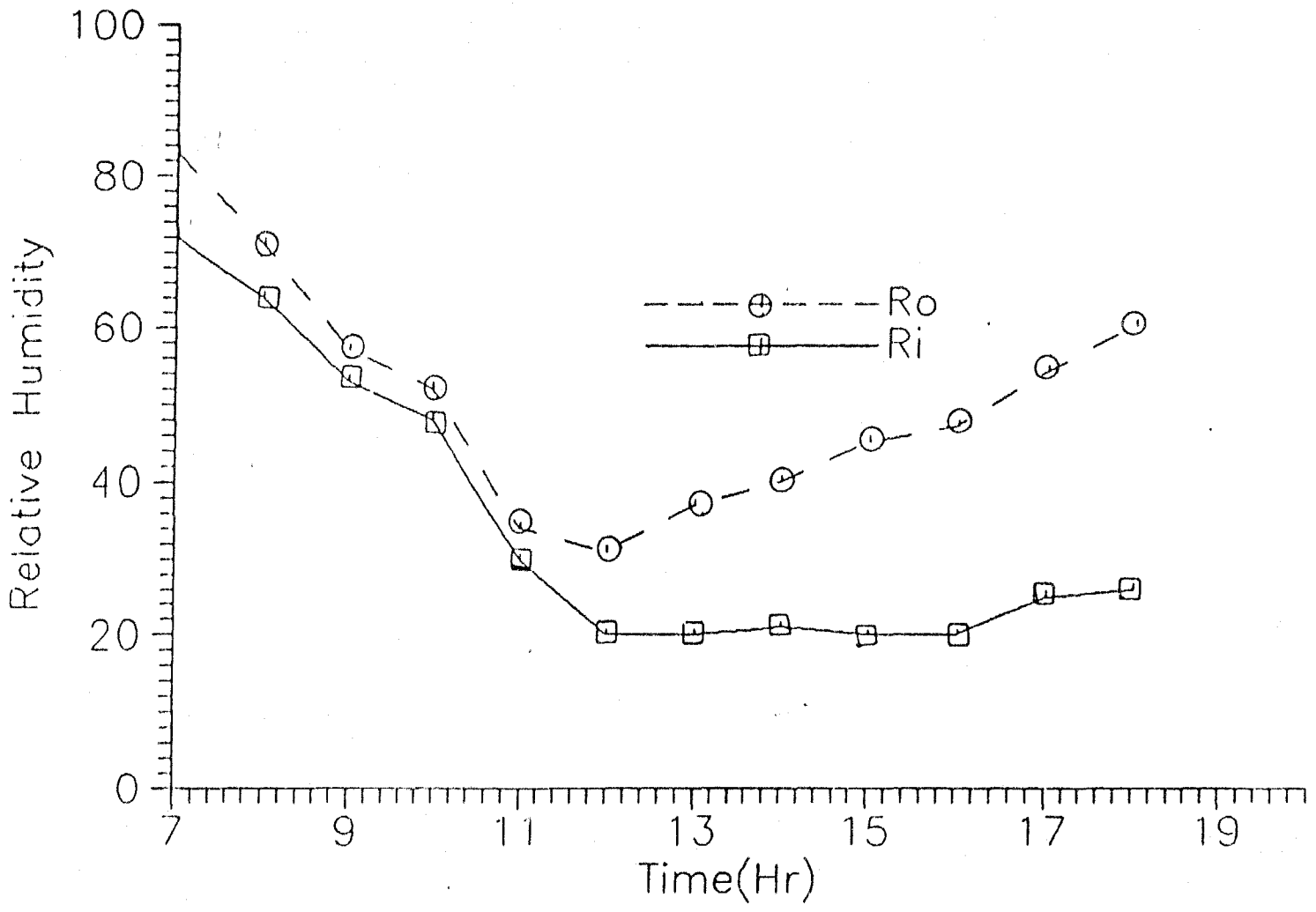

Fig: 6.13 Measured value of Relative Humidity in solar dryer.
(Natural Air Flow Configuration)

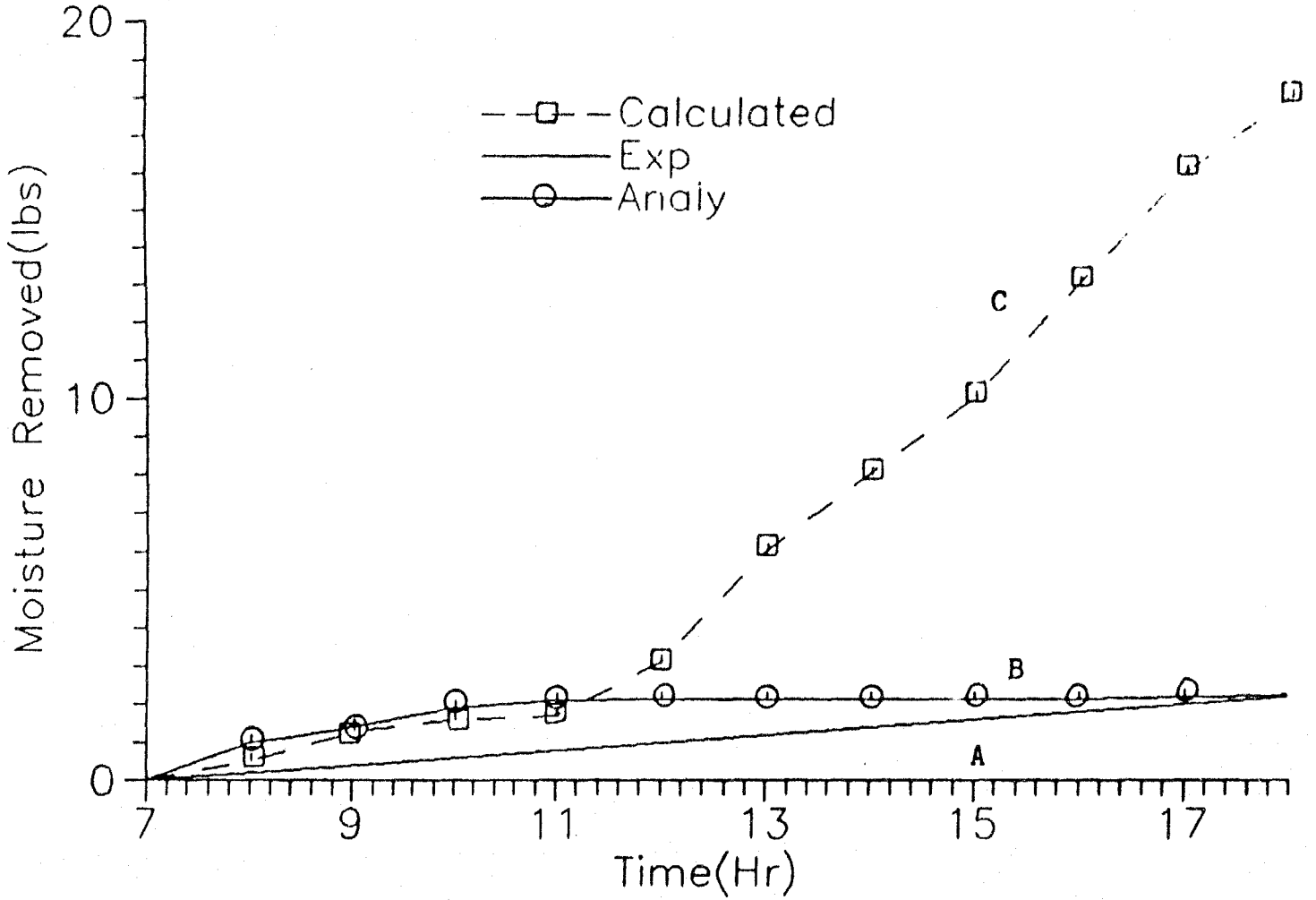

Fig: 5.14 Cumulative amount of moisture removed with respect to time(Analytical & Experimental) (Natural Air Flow Configuration)

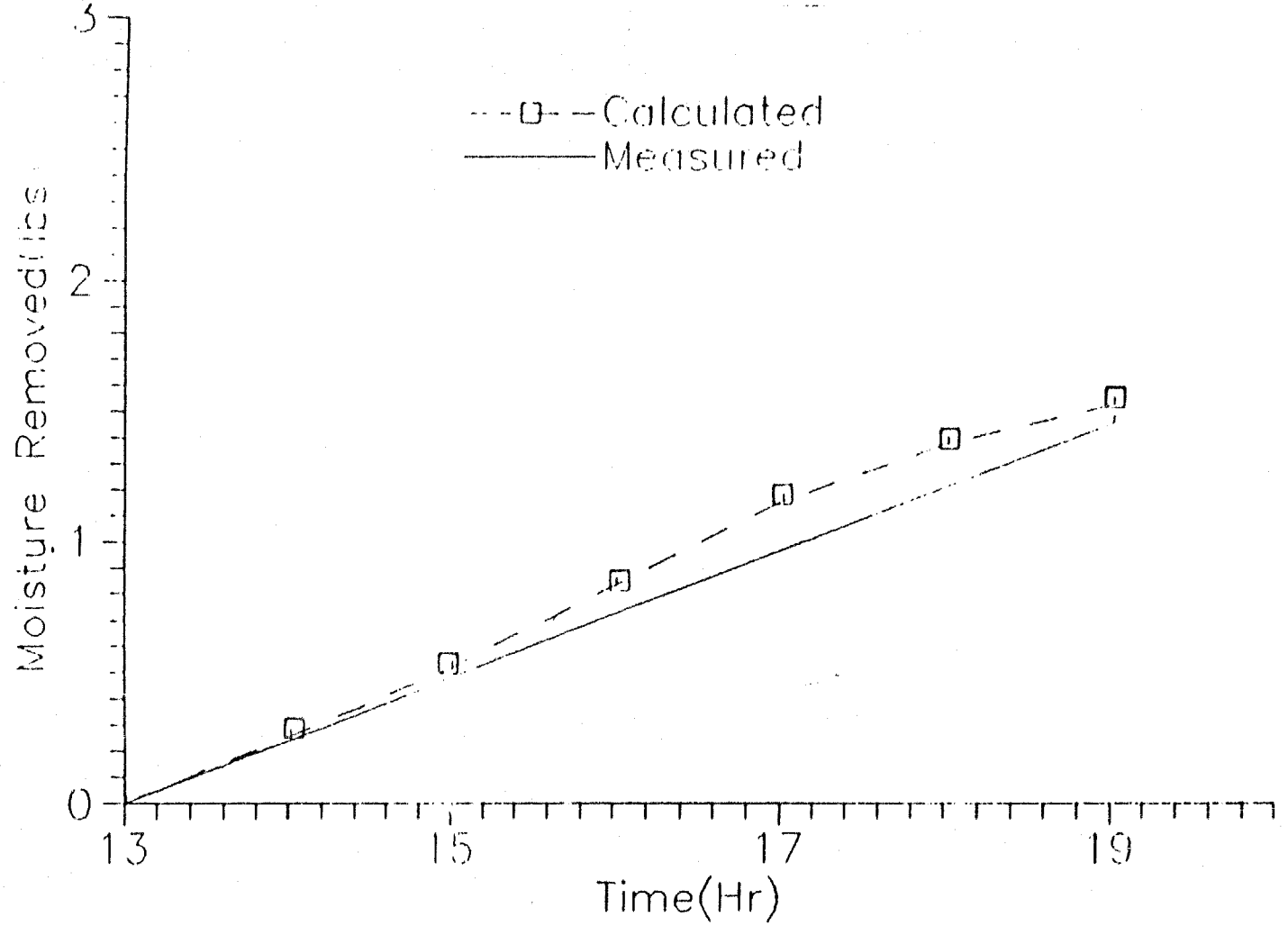

Fig: 5.15 Measured and calculated values of moisture removed from grapes.(Calculated values from Air and RH)

REMARKS ON DIFFERENCE BETWEEN THEORETICAL AND EXPERIMENTAL RESULTS:

Refering to figures 6.8 and 6.14, it is seen that there are large differences between the curves A and C. Curve C represents the moisture loss calculated from the temperature, the humidity and the flow measurements of the air. The following may explain the reasons for the error in the curve C.

1. The air may have picked moisture from the ground. It was also observed that the structural wood absorbed the moisture during the night time which was removed by the air during the daytime.

2. Error in the instruments during recording of data.

To find out the extent of the instrumentation error, another set of data were recorded in which temperature and humidity sensors were put just above and below the tray. Figure 6.15 shows the comparision. Both the curves are fairly close. It means that most of the difference in the curves A & C can be accounted for by moisture in the exit air from sources other than the grapes.

The difference between curves A and B can be explained as follows:

1. The drying equations are based on a thin-layer drying concept. The thin layer dries uniformly and at the state conditions defined by figure 6.16. No gradients of properties through the layer are assumed. This does not hold, however, for a finite mass depth.

2. The air temperature, relative humidity and specific volume change as the air moves through the finite mass. The change in the state of the air causes a progressive change in the drying rate because the temperature change affects the diffusivity, the relative humidity affects the equilibrium moisture content, M(e) and the change in specific volume affects the mass flow rate.

3. Equations are based on a uniform half thickness "a" of grapes. However, in our case the depth of grapes was not uniform.

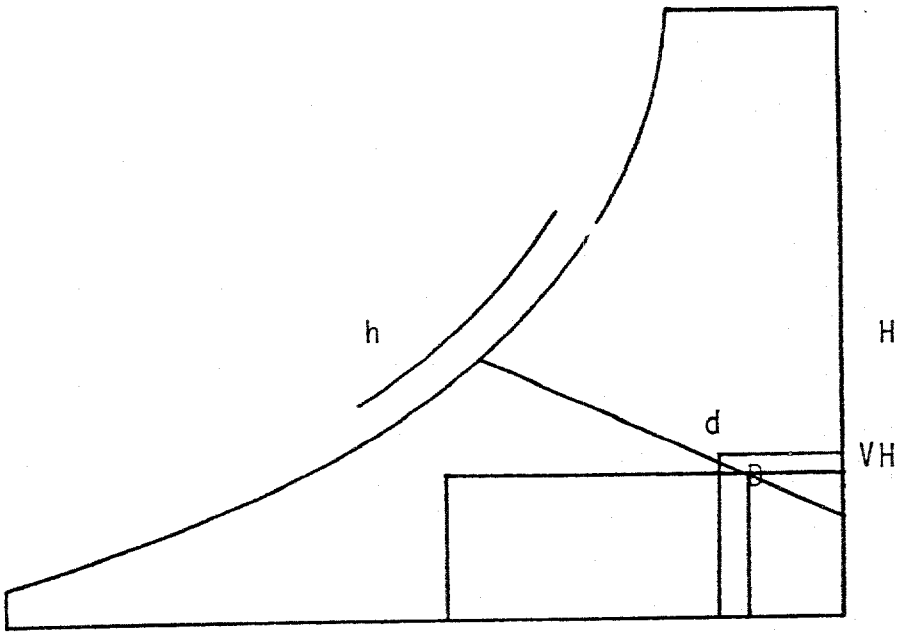

Fig: 6.16 The air state change b to d for a drying process.

CHAPTER 7
CONCLUSIONS

Geodesic dome type structure can be easily built with wood or bamboo, in short time, and is economical because wood is cheap and available in most parts of the world.

Tests showed that a geodesic solar dryer requires 7-8 sunny days to dry grapes. Results between the two experiments showed that a Natural Air Configuration with a ventilator is a better choice than a Forced Air Configuration. Tables 6.2 and 6.5 show that the moisture removed is almost the same and it is convenient for the developing countries where electricity is not available in some parts.

Data from the tables indicates that the ground moisture has significant effect on the drying process. For efficient drying, the moisture release from the ground should be minimized by covering the ground.

REFERENCES

1. Lawand, T.A., "A Solar Cabinet Dryer", Solar Energy, 10 (4), 158, 1966

2. Gutierrez- Medina, J. A.,"Adoptive Use of Greenhouse Structure for Fruit Drying", M.S. Thesis, University of Arizona, Tuscon, AZ., 1981

3. Huang, B. K. and Bowers, C.G.,"Development of Greenhouse Solar Systems for Bulk Tobacco Curing and Plant Production", Energy in Agriculture, 5, 267-284, 1986

4. Cruss, W. V. and Christie, A. W., "Some Factors of Dehydrator Efficiency", California Agriculture Experiment Station, Bulletin 337: 284-287, 1921

5. Christie, A. W. and Nichols, P.F., "The Dehydration of Prunes", California Agriculture Experiment Station, Bulletin 404: 10-19, 1927

6. Mark, E. M.,"Dehydration of Fruits", Agriculture Engineering 19: (8) 349-352, 1938

7. Genrty,J. P., Miller, M. W. and Claypool, L. L.,"Engineering and Fruit Drying Aspects of Prune Dehydration in Parallel and Counter-flow Tunnels, Food Technology, 19:(9), 121-125, 1965

8. Robert, A. Parsons, Parallel Flow Fruit Drying, 1968

9. Rodda, E. D. and Gentry, J. P.,"New Concept in Fruit Dehydration Construction", Transaction of ASAE, 12: (4), 540-542, 1969

10. Cheng, P. K., Control of Flow Seperation, McGraw Hill, New York, 1976

11. Groh, J. E.,"Energy Conservation in Fruit Dehydrators Utilizing Recirculation of Exhaust Air and Heat Recovery Heat Exchangers", Final Report for contact No.E (11-1) -2916, U.S. Energy Research and Development Administration, 1978

12. Carnegie, E. J., Heat Recovery on a Tunnel Dehydrator. Paper presented at the ASAE meeting in San Antonio, TX, June 15-18. Paper

13. Thomson, F. J., Chinnan, M. W., and Knutson, G. D., "Energy Conservation of Drying of Fruits in Tunnel Dehydrators", Journal of Food Process Engineering, 4, p.155-169.

14. Adam, "Types of Solar Agricultural dryers", Sunworld, 4. (6), 181, 1980

15. Paschkins, V ,"Periodic heat flow in building walls determined by electrical analogy method", Trans. ASHVE 48:75-90, 1942

16. Paschkins, V. and Baker, H.D. , "A method for determining unsteady-state heat transfer by means of an electrical analogy", Trans. ASME 64: 105-112, 1942.

17. Nottage, H.B. and Parmelee, G.V. "Circuit analysis applied to load estimating. Trans. ASHVE 60: 59-102, 1954.

18. Buchberg, H.," Electrical analogue prediction of the thermal behavior of an inhabitable enclosure. Trans. ASHVE 61: 339-386, 1955.

19. Jenson, W.R. and Lieberman, M.D.,"IBM electronic circuit analysis program (ECAP) techniques and applications. Prentice-Hall Inc., Englewood Cliffs, N.J., 1968.

20. Huang, B.K.,"Digital simulation analysis of biophysical systems", Trans. IEEE BME-19(2): 128-139, 1974.

21. Huang, B.K.,"Electronic circuit analysis program application", Agriculture Engineering, 55(7) :52, 1974.

22. Jordan, K.A., Huang, B.K. and Magee, C.,"ECAP in agriculture engineering, teaching and research", Trans. ASAE 18(3) : 596-600, 1975.

23. Huang, B.K.,"Dynamic system analogies and mathematical interpretation", ASAE winter meeting, Dec. 11-14, paper no. 73-5549, 1973.

24. Huang, B.K. and El-Shaik, N.M., "Simulation analysis of greenhouse solar drying system for peanuts and grains", ASAE 1979 summer meeting, paper no. 79-3082, 1979.

25. Ozisik, N.M. and Huang, B.K., "Utilizing of solar energy in grain drying", Final Report,North Carolina Energy Institute, Research Triangle Park, N.C. 27709, July 1979.

26. "Dome Book 1", Shelter Publications, Box 279, Bolinas, CA

27. "Dome Book 2", Shelter Publications, Bolinas, CA

28. "Shelter II", Shelter Publications, Bolinas, CA

29. Henderson, S. M. and Perry, R. L.,"Agricultural Process Engineering", AVI Publishing, Westport, CT 06880